CZECH TECHNICAL UNIVERSITY IN PRAGUE

FACULTY OF ELECTRICAL ENGINEERING

Department of Electrical Power Engineering

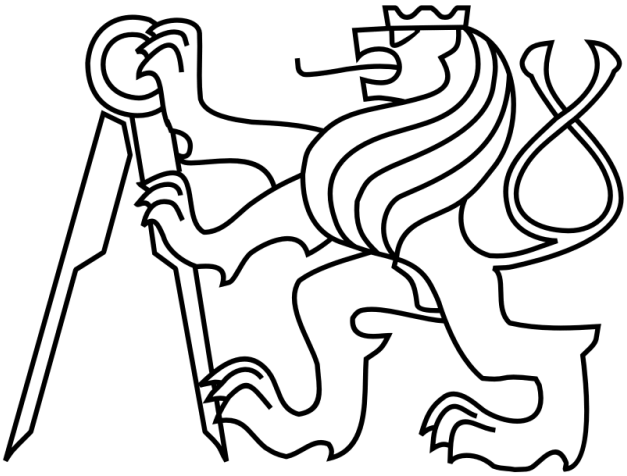

DIPLOMA THESIS

Measurement of Losses at Low Power Factors

Bc. Michael Schneider

Thesis Supervisor: Ing. Radek Procházka, Ph.D.

Study Programme: Electrical Power Engineering

Prague 2015

Acknowledgements

In the beginning, I would like to express my thanks to Radek Procházka for topic for working and for his professional assistance during real measurements.

At this point, I feel also obliged to thank Associate Professor Jan Kyncl because an important part of this thesis is based on his work. I would also like to express my gratitude to my proofreader, Nicholas Edwards, for his corrections, which gave the thesis its final linguistic form and from whom I learned something new. Moreover, I thank Petr Javorik for his careful final reading. I appreciate his attitude, especially as he told me he was looking forward to reading what I have written. Last but not least, my most heartfelt thanks go to my family. I would not be able to present this thesis without their support.

Affidavit

“I hereby declare that I wrote the presented thesis independently and I quoted all information sources in accordance with the Methodical instructions on ethical principles during the preparation of this academic thesis. “

Čestné prohlášení

„Prohlašuji, že jsem předloženou práci vypracoval samostatně a že jsem uvedl veškeré použité informační zdroje v souladu s Metodickým pokynem o dodržování etických principů při přípravě vysokoškolských závěrečných prací.“

V Praze dne: ……

České vysoké učení technické v Praze
Fakulta elektrotechnická

katedra elektroenergetiky

ZADÁNÍ DIPLOMOVÉ PRÁCE

Student: **Michael Schneider**

Studijní program: Elektrotechnika, energetika a management
Obor: Elektroenergetika

Název tématu: **Měření činných ztrát při malých účinících**

Pokyny pro vypracování:

1) Popis metod pro měření činných a jalových výkonů u vysokonapěťových zařízení.
2) Realizace měřicího systému pro stanovení činných ztrát při malých účinících.
3) Ověření přesnosti jednotlivých metod laboratorním měřením.

Seznam odborné literatury:

[1] HAASZ, Vladimír a Miloš SEDLÁČEK. Elektrická měření: přístroje a metody, Vydavatelství ČVUT, 2005
[2] Djokic, B.; So, E., "The development of a digital sampling systém for low power factor measurements of high-voltage capacitive/inductive reactors," Instrumentation and Measurement, IEEE Transactions on , vol.54, no.2, pp.604,607, April 2005

Vedoucí: Ing. Radek Procházka, Ph.D.

Platnost zadání: do konce letního semestru 2015/2016

L.S.

Ing. Jan Švec Ph.D.
vedoucí katedry

prof. Ing. Pavel Ripka, CSc.
děkan

V Praze dne 1. 4. 2015

Abstract

Předložená práce je zaměřena na problematiku měření činného výkonu při malém účinníku. V úvodu jsou popsány jednotlivé metody měření ztrát při malých účinních, přičemž je kladen důraz na popis dvou metod číslivového zpracování, jejichž teoretické a praktické porovnání je hlavní náplní této práce. Podstatná část práce se zabývá speciálními měřicími transfromátory a také metodami číslicového zpracování, zejména pak určením periody měřeného signálu.

Klíčová slova

Měření výkonu, systém pro měření výkonu, měření činného výkonu při malém účinníku, měření ztrát.

Abstract

The presented thesis is focused on active power measurement at a low power factor. The introduction describes the various methods for the measurement of losses at low power factors with the emphasis on two techniques of digital signal processing. The theoretical and practical comparison of these methods is the primary concern of this work. A significant part of the thesis deals with two-stage transformers and also with zero-crossing detection algorithms.

Keywords

Power measurement, power measurement system, active power measurement at low power factor, measurement of losses.

Contents

1. Motivation

The primary motivation for measuring active power at a low power factor is to determine power losses. During the transmission and distribution of electricity, some electrical energy is lost from the system, usually in the form of heat. This lost energy is known as technological own power consumption. The losses from power transformers and reactors are part of these losses. Technological own power consumption is defined by the Czech Energy Regulatory Office [1] as: Consumption of electrical energy for electricity production, or for the production of electricity and heat in the main production facility and its auxiliary operations which are directly related to the production of electricity or electricity and heat. This power consumption is composed of losses during the production, conversion or modification of fuel, losses related to wiring for own consumption, losses from transformers, and losses from overhead lines and cables in a grid.

Technological own power consumption is paid for by all electricity consumers. It is one of the components of electricity pricing. The fee for technological own power consumption is included in the fee for maximum power consumption (limited by a circuit breaker), and in the fee for the amount of electricity consumed. These two components are related to the distribution of electrical energy. The last part is a fee for system services, which are charged to ČEPS a.s. This fee is related to electricity transmission.

The aim of defining technological own power consumption is to divide the costs of the production, transmission and distribution of electricity among all users. These costs are not only composed of technical costs, but also include non-technical costs such as personnel costs, the maintenance of existing facilities, or purchase of new equipment. The question of how to divide technical costs in the power grid among users is a really interesting one due to the physical nature of losses (losses increase with the square of the load current). Neither technical nor non-technical costs can be shared fairly among all users.

The main parameter of a reactor or capacitor is its reactive power. Active power represents losses, but for many machines and other facilities these losses may not be known. Losses can be determined by calculation or by measurement. The estimation of losses by calculation is a standard part of the manufacturing of large reactors or transformers. After the machine is manufactured, the calculated losses are compared with the measured losses. This process plays an important part in the development of new products.

In his article ‘A Technique for Calibrating Power Frequency Wattmeters at Very Low Power Factors’ [2], pointed out an important fact - that an increase of losses is not directly proportional to an increase of apparent power. He also gives examples of a few typical values: ‘‘A shunt reactor with a 50 Mvar rating might have a power factor of 0.4 percent while another with a 100 Mvar rating would have a power factor of 0.2 percent.’’ The losses of large power transformers are also mentioned. The power factor is not

usually so small, but is still approximately 1-2 percent. The losses of these machines remain almost constant with increasing apparent power, which makes the measurement of these losses even more difficult.

There are many ways to measure losses. I would like to divide all of these methods into two groups. The first group is represented by calorimeters, which is a method based on the measurement of non-electrical values. Losses are predominantly represented in the form of heat and this encourages the use of calorimetric apparatus. The calorimetric apparatus has been designed almost exclusively for the measurement of losses in capacitors [3]. Another use for calorimeters in Electrical Engineering is for measuring the losses of amplifiers' output stages. These examples represent small electronic devices or instruments. The development of calorimetric apparatus to measure transformers and shunt reactors, or other bulky machines which operate at a high voltage, is unrealizable.

All of the methods in the second group are various types of electrical measurement. These include bridge methods, calibrated analog wattmeters, power analyzers and other special measuring devices such as high voltage wattmeters [4]. Each approach has its particular advantages. The final decision as to which method is best depends on the particular circumstances. For instance, in the case of laboratory measurement, the best results are realised with bridge methods. These methods require a sizable normal capacity, which limits their use for a wider range of measurement.

These days, measurement is mostly performed by digital instruments. Analog wattmeters are gradually being replaced by digital wattmeters and power analyzers. Digital processing techniques have many advantages. Moreover, the disadvantages are increasingly suppressed due to progress in the computer technology world. The price of these instruments is also going down. Consequently, digital measurement is the leading technique today and has no real competition.

2. Methods of measuring losses

2.1. The average value over a period of the instantaneous power

2.1.1. Theoretical analysis

Naturally, the first method of choice is the calculation of active power as the average of the instantaneous power. It is also used to define active power for an alternating system. In real cases, we work with sampled and quantized discrete values. At first there are sources of uncertainty because we know nothing about the voltage of the resp. current between samples. Quantization errors depend on the number of bits of an analog-to-digital converter.

Active power for continuous variables is:

$$P_c = \frac{1}{T}\int_{t_s}^{t_s+T} p_i(t)\,dt = \frac{1}{T}\int_{t_s}^{t_s+T} u_i(t)i_i(t)\,dt \qquad (1)$$

Index i means that values are instantaneous. For discrete variables, integral changes to the sum of discrete values:

$$P_d = \frac{1}{N}\sum_{k=1}^{N} p_i(k) = \frac{1}{N}\sum_{k=1}^{N} u_i(k)i_i(k) \qquad (2)$$

This is the arithmetic average of the sum of products. It is a basic equation used by power analyzers to determine active power. It also defines active power for discrete values. This method is simple and robust. The figure below shows the waveforms of voltage, current and instantaneous power for the inductive load. The green-dashed line represents the active power.

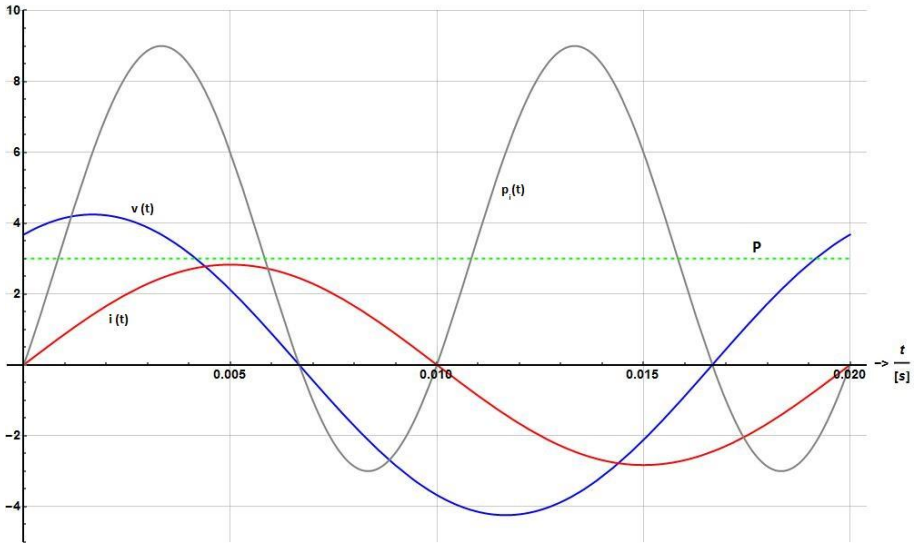

Figure 1. Active power

Figure 2. shows two waveforms of instantaneous power. The grey waveform represents continuous instantaneous power and the purple points represent discrete samples. Each sample is a product of the voltage and current sample at that moment. This calculation is problematic as the final error does not only depend on the quantization errors of the current and voltage, but on a combination of both errors. As you can see, some samples in Figure 2. do not really fit onto the grey reference line. These samples are the result of a calculation in which both current and voltage samples were rounded down and up respectively. For instance, the ninth sample is fairly low, and there are also some samples which are too high. However, despite this problem, the total error is not so big due to the large number of samples. In real cases, there are several hundred or thousands of samples for one period. The final value of the active power is the sum of all these samples during the period. The errors are not just positive or negative; therefore, the calculated result is not too bad. In fact, the result is surprisingly accurate, even for a relatively under-sampled signal. The choice of the sampling frequency is a complex question, which I will describe in more detail later.

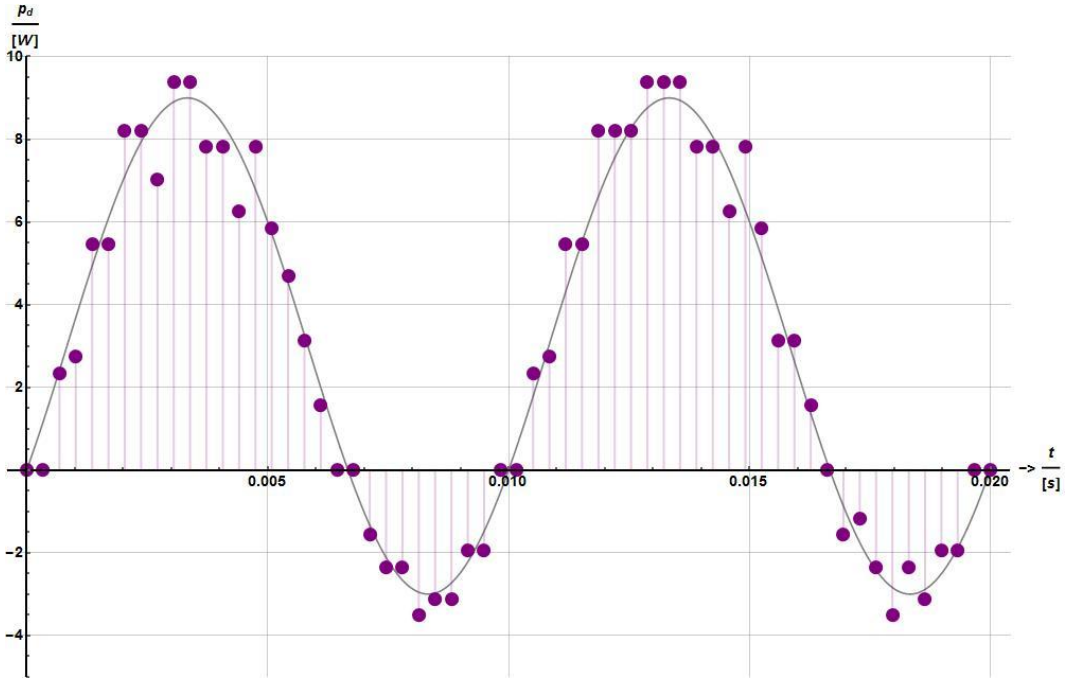

Figure 2. Instantaneous power error

The Figures above show waveforms that are typical for an inductive load in a harmonic steady state. The power factor in this expamle is 0.5, which implies that the phase angle is 60^o. At this point I would like to mention two extreme cases of instantaneous power waveforms: firstly, when the phase angle is 0^o, the respective power factor is 1. In this case, the load is free from the reactive component. The instantaneous power can be described by the following equation:

$$p_i = P_{max} \sin^2(\omega\, t) \tag{3}$$

The active power is the average value over a period:

$$P = \frac{1}{T}\int_0^T P_{max}\ \sin^2(\omega\,t) = \frac{P_{max}}{2} = \frac{U_{max}\,I_{max}}{2} = U * I \qquad (4)$$

The active power is the product of the effective values of the current and voltage.

Secondly, when the phase angle is 90°, the respective power factor is 0. This represents an entirely reactive load. For this condition, the instantaneous power is as follows:

$$p_i = \frac{P_{max}}{2}\ \sin(2\ \omega\,t) \qquad (5)$$

Obviously, the active power is zero:

$$P = \frac{1}{T}\int_0^T \frac{P_{max}}{2}\ \sin(2\ \omega\,t) = 0 \qquad (6)$$

2.2.1. Active power measurement error

I dealt with active power measurements and digital processing in my Bachelor thesis. Here I present two graphs which show active power errors when a trapezoidal method is used to calculate the avarage value from the instantaneous power. The accuracy of this method is affected by many influences – some of them are obvious, but others are more complicated. Firstly, the precision of the method is directly proportional to the effective range and number of bits of analog to digital converters, which is not surprising .The bit resolution is fixed, but the next thing is to use the entire range of the converter.

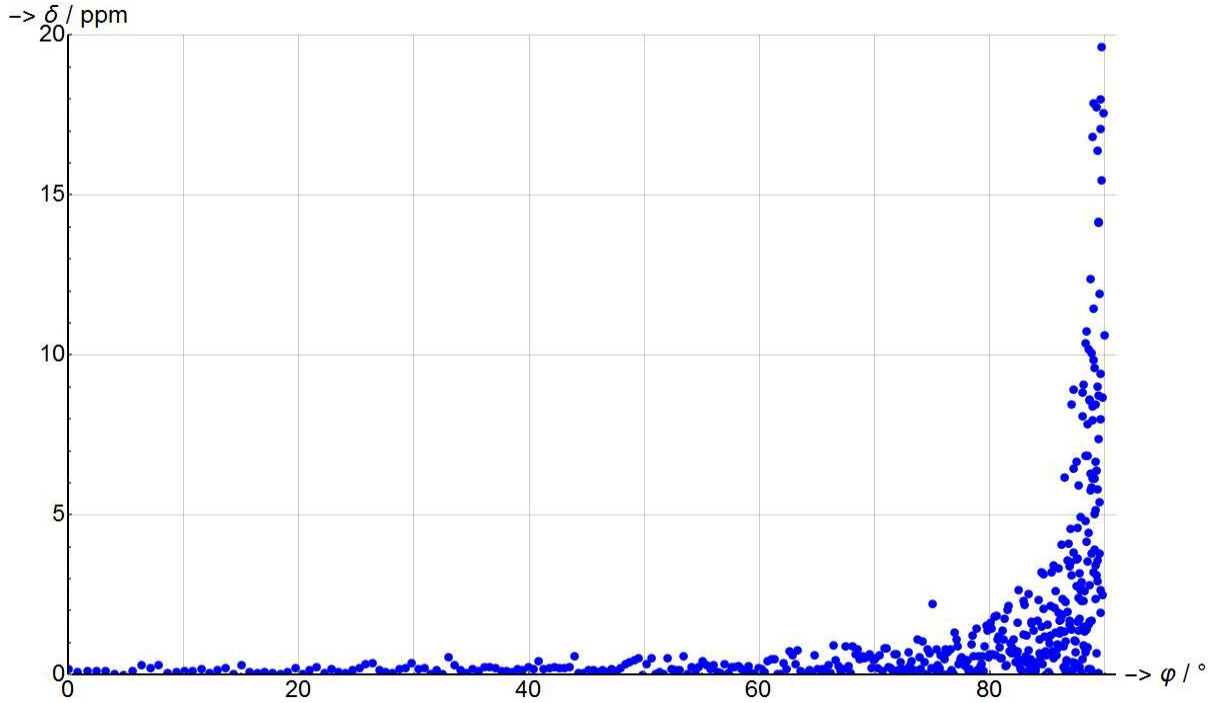

Figure 3. Active power measurement error

Secondly, the accuracy may also depend on the method of numerical integration. I will focus on the differences between the trapezoidal method and Simpson's rule. Generally, it depends on the ratio of the measured frequency and sampling frequency. If the sampling frequency is much higher than the frequency of the sampled signal, the difference is negligible [19]. Using a lower sampling frequency requires Simpson's rule [24]; however, a significant difference begins to emerge with a sampling frequency of 2 kHz for a 50 Hz sampled signal. In practice, the sampling frequency is at least several tens of kHz or higher.

Thirdly, the correlation between the sampling frequency and the accuracy may be disputed. By this I mean very high sampling frequencies in real measurements when the signal is very oversampled, as then the error may depend mainly on the zero-crossing detection algorithm. For the mathematical model, which was created in the bachelor thesis, it is true that the higher sampling frequency corresponds with higher accuracy, but only because the program was working within a specified period. Unfortunatelly, white noise may play a role in a period's determination, which can then cause the biggest error. Therefore, a very good zero-crossing algorithm is needed.

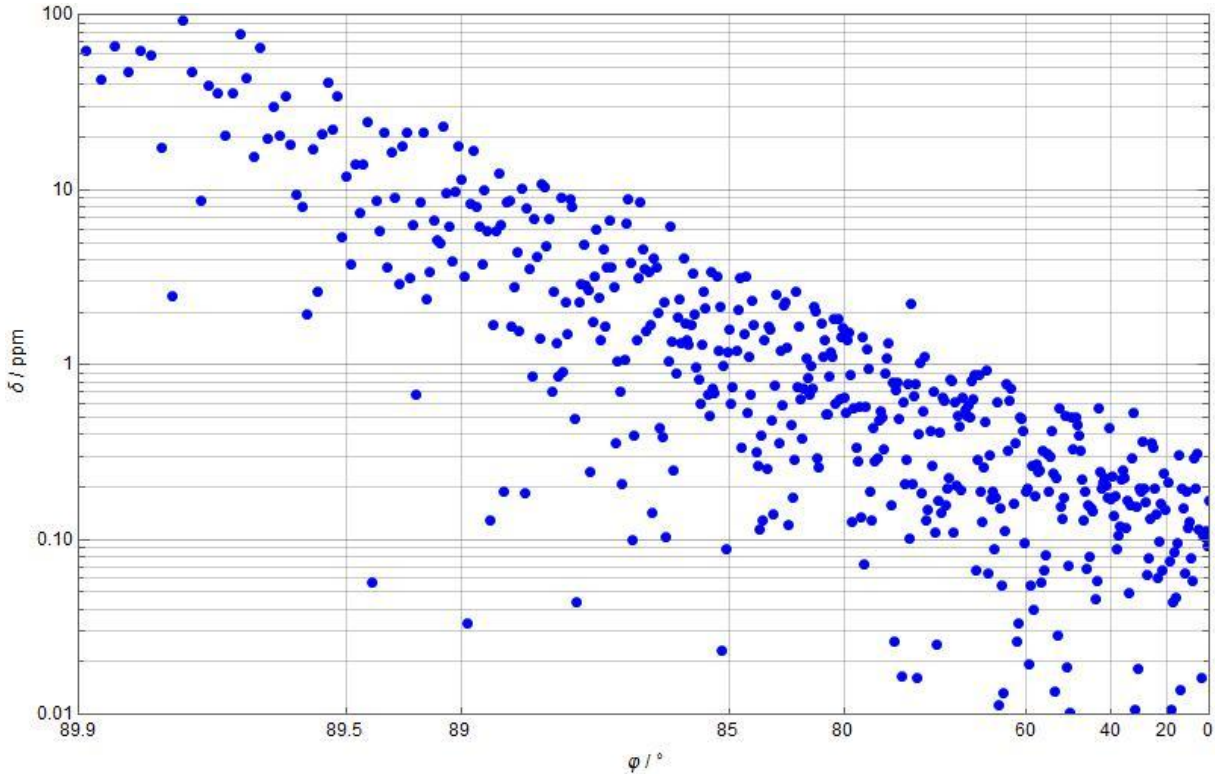

Figure 4. The active power error - inverse logarithmic scale

The second graph shows the same dependence of error with the phase angle, but this time on an inverse logarithmic scale which is more suitable to capturing its whole range. The graph shows that an error at low power factors is approximately a thousand times greater than an error when the power factor is close to one. This is described in detail with all parameters in [19].

2.2. Active power calculation based on phasors measurements

2.2.1. General overview

In 1893, the mathematician and electrical engineer Charles Proteus Steinmetz presented a paper on mathematical techniques for analyzing waveforms of current and voltage in alternating systems. In his paper, Steinmetz used the concept of phasor for the simplification of alternating quantities in harmonic steady-state. This concept found use in many branches of science, and especially in Electrical Engineering. All current techniques concerning phasors are based on his work.

More recently, the calculations for synchronized real-time phasor measurements were developed. Nowadays it is frequently discussed as problematic because of the new requirements of grid management. Existing installations are not able to secure dynamic monitoring of the grid because they are not able to capture the data at the same time. In contrast, synchronized phasor measurements are based on precise time synchronization, because when time is precisely synchronized it is possible to put all obtained phasors on the same phasor diagram. It is a powerful tool not only for monitoring, but also for controlling and protecting the grid. The future importance of the method is captured in this statement by Terry Boston, CEO of PJM Interconnection: "It's like going from an X-ray to an MRI of the grid." [20].

2.2.2. Phasor measurement unit

The basic building unit for a monitoring system which uses the measurement of synchronous phasors is a phasor measurement unit (PMU). The structure of a PMU based on a DSP is shown in the following figure [21].

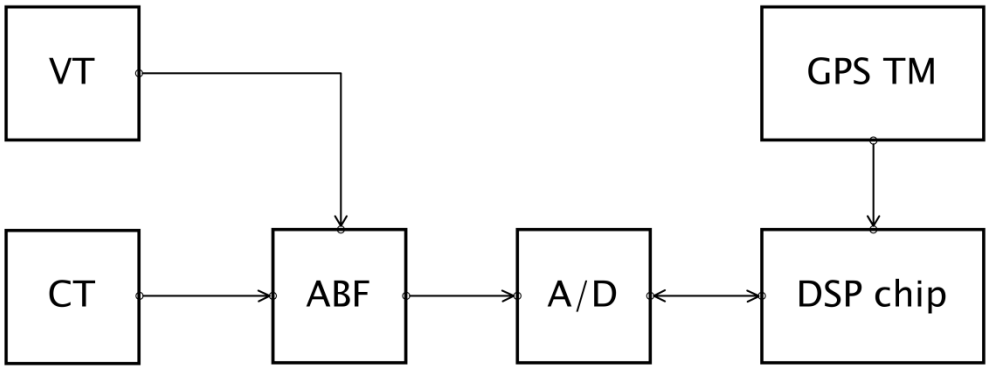

Figure 5. Phasor measurement unit

The instrument transformers (VT and CT) convert the voltage and current to a workable level. ABF stands for analog band-pass filter, with a frequency of f_0 = 50 Hz and a bandwidth of 10 Hz because the PMU works with fundamental signals. The voltage and current are converted to discrete values in an analog-to-digital converter (A/D) and are

processed in the DSP unit with respect to the time reference, which is obtained from a GPS timing module (GPS TM). The complete software process is described in more detail in [21].

Precisely measured phasors of voltage and current are not the only outputs of the PMU. Their measurements enables us to calculate the active and reactive power flow as well as the frequency. The challenges associated with accurate phasor measurement are similar to the problems with the precise measurement of losses. Zero crossing and discrete Fourier transform (DFT) are the most important methods affecting the accuracy of phasor measurement. There is a difference in the DSP because in the previous method it is just a calculation of the mean value. Nevertheless, the challenge of determining the period is the same.

2.2.3. Specific method description

The numerical method for phasor calculation is based on the article 'On measurement of synchronous phasors in electrical grids', which was written at CTU FEE by Associate Professor Jan Kyncl, Adithya Hariram and Martin Novotný [5]. It is a sophisticated method for phasor determination and frequency assessment, and I am using its modified extension that is suitable for power measurements. Active power measurements were not the primary goal of this method, but during consultations with my supervisor it became clear that this method has the potential to achieve good results; therefore, I was asked to compare such method with classical methods that use zero crossing detections and trapezoid integration of the discrete samples within a period.

Evidently, the direct output of the integration of the instantaneous power samples over a period is the active power, while the results of this other method is the phasor voltage or phasor current respectively. The active power from these phasors is possible to calculate using the following formula:

$$P = \hat{U}\,\hat{I}^{*} \tag{7}$$

Since we can calculate only the active power of the first harmonic this way, the method is extended to determine forty harmonics and the active power is calculated from all of them. I suppose that the active power is composed of products of voltage and current with the same frequency [19, 28]:

$$P_{total} = \sum_{i=1}^{40} \widehat{U_i}\,\widehat{I_i}^{*} \tag{8}$$

I have limited the number of harmonics to forty as it is the most common value used in practice and it is sufficient for the waveforms that occur in Electrical Power Engineering.

The proposed method [5] for phasor measurements and frequency assessment uses the following formula:

$$x = \frac{1}{L} \int_{t = t_0}^{t_0 + L} f(t)\, dt \tag{9}$$

Generally, the mean value x depends on the beginning and the length of the interval. We can expect intervals of length L = T for which it is true that the mean value x is independent of t_0 and is a constant for any value of t_0 . In contrast, the mean value of intervals with different lengths varies with t_0. The differences of these intervals are described by standard deviation σ. If the mean value is a constant (for sine wave zero) then the standard deviation is zero and length L is exactly the length of the period of the observed signal [5].

In this method, we chose length L and then calculated the mean values x for several different t_0. Then we calculated the standard deviation σ. However, in practice, we are working with a discrete signal which is represented by samples. Because of this, it is necessary to create several sampling windows, and for each of them to evaluate the standard deviation. Then we calculated the minimum from these several values, and thus we determined the exact frequency. A complete description of this method is given in [5]. If we have determined the period of the first harmonic component, we can calculate coefficients of Fourier series [5]:

$$a = \frac{2}{T} \int_0^T s(t) \cos\left(2\pi \frac{t}{T}\right) dt \tag{10}$$

$$b = \frac{2}{T} \int_0^T s(t) \sin\left(2\pi \frac{t}{T}\right) dt \tag{11}$$

From which we get the phasor that represents the first harmonic component:

$$\hat{S} = a + jb \tag{12}$$

Other harmonic components are possible to calculate according to the following formulas, while the **n** is an integer from 1 to 40:

$$a_n = \frac{2}{T} \int_0^T s(t) \cos\left(2\pi \frac{t}{T}\, n\right) dt \tag{13}$$

$$b_n = \frac{2}{T} \int_0^T s(t) \sin\left(2\pi \frac{t}{T}\, n\right) dt \tag{14}$$

The results are phasors for each harmonic component under consideration according to equation (12).

2.3. Other methods of measuring active power at low power factor

2.3.1. Vector voltmeter

Another promising method is the vector voltmeter. This electronic device has two AC inputs and one DC output. The vector voltmeter is based on a controlled rectifier (CR in Figure 6.), which is sometimes called a phase-sensitive rectifier. The controlled rectifier is controlled by the reference voltage, which can be shifted by 90^o in the phase shifting block. The reference voltage is changed in the squaring circuit (SC) to a square wave in order to clearly define the zero crossing. The switch position selects which reference voltage is used to control the rectifier. Depending on the reference voltage, the controled rectifier realises part of the unknown voltage U_x. Filter (F) filters out the AC component and the output DC voltage is proportinal to the real part of the phasor (the switch‘s position is 0^o), and respectively for the imaginary part when the shifted voltage is used (the switch‘s position is 90^o) [10].

This method is actually quite similar to the phasor measurements because the result is a phasor. The vector voltmeter is a very sophisticated instrument and has many different uses. It can be either analog or digital.

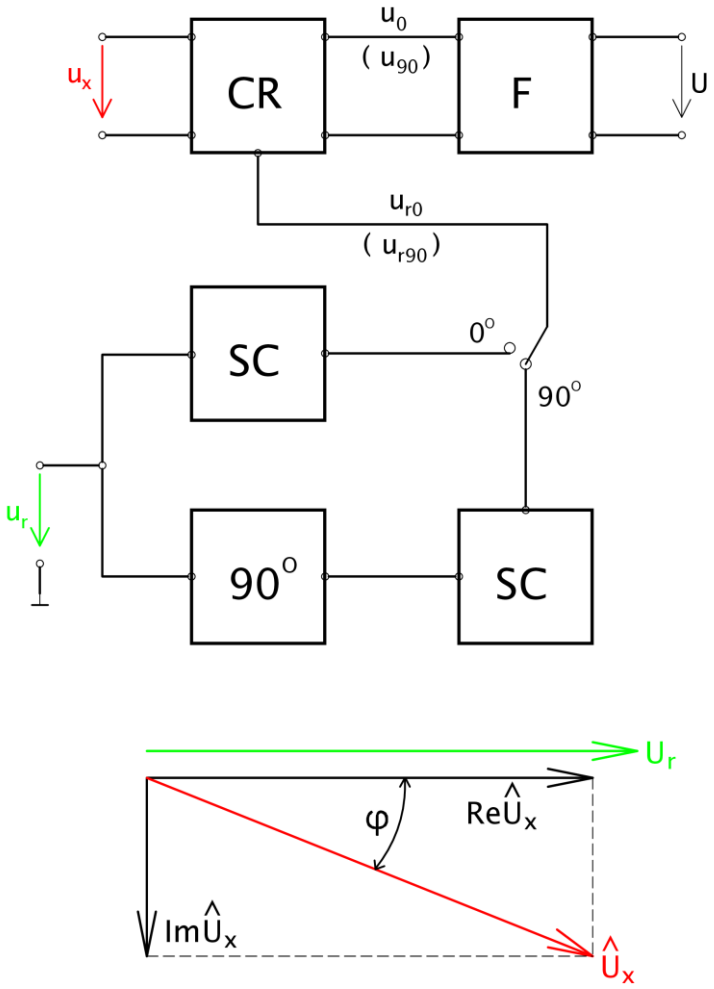

Figure 6. Block and phasor diagram of the vector voltmeter

2.3.2. Analog wattmeters

Analog wattmeters have been replaced by digital wattmeters and power analyzers, but this was a leading technique for many years. The theory of measurements at a very low power factor by analog wattmeters is based on their detailed analysis. The active power measured by an analog wattmeter does not only depend on the product of the voltage and current with respect to the phase angle. In fact, it may depend on the voltage and current alone, or on the product of the voltage and the quadrature component of the current. These dependencies cause other errors which must be added to the unity power factor error according to the following equation [2]:

$$P = (1 + k_P)VIcos\varphi + k_q VIsin\varphi + k_V V^2 + k_I I^2 \quad (15)$$

Where P is the measured active power, V is the voltage, I is the current and φ is the phase angle.

- k_p represents the unity power factor error
- k_q is the zero power factor error
- k_v and k_I describe the sensitivity to voltage and current

Further measurement is needed for determination of these coefficients. In the article 'A Technique for Calibrating Power Frequency Wattmeters at Very Low Power Factors' the calibration circuit for their measurement is described. For instance, it is possible to determine the voltage coefficient when the voltage is applied to the wattmeter and the current terminals are open. Other coefficients are determined similarly. The calibration circuit mentioned in the article is used for electrodynamic wattmeters as well as for electronic wattmeters [2].

2.3.3. AC Bridges

AC Bridges are typically various modifications of the Wheatstone bridge. They can be used to measure capacity, inductance, permeability and the loss angle or dissipation factor. For instance, the dissipation factor measurement is usually performed using bridge methods. It is one of the diagnostic methods for high voltage apparatus. The condition of the insulation of these apparatus may be monitored as the dissipation factor grows with time. The dissipation factor is the tangent of a loss angle, which is a supplementary angle to a phase angle, and is usually very small. It is related to dielectric losses by the well known formula:

$$P_d = U^2 \omega C \, tan\delta \quad (16)$$

P_d represents losses in power transformer insulation, dielectric losses in cables, or other losses of capacitive loads. Knowledge of dielectric losses is significant for high voltage apparatus as such losses depend on the square of the voltage. To measure these apparatus, the Schering Bridge is often used, which, in my opinion, is the most sophisticated bridge method. In addition to the dissipation factor, the capacity and permeability are also often measured. The circuit for the measurement of the dissipation angle is described in [6].

For the measurement of inductive loads, a Maxwell-Wien Bridge [7] may be used. Similar to the Schering bridge, there are numerous modifications that improve the basic bridge for specific uses [8]. In fact, the Maxwell-Wien Bridge is used less often than the Schering Bridge. The measuring of capacitive loads is far more prevalent.

The biggest advantage of AC bridges is their accuracy. Measurements using AC bridge methods may be used to check capacity or inductance references. However, AC bridges have many disadvantages. When the supply voltage is within reasonable limits, the realised value is independent of the amplitude of the supply voltage, but an unsuitable choice of supply voltage may cause problems during balancing. AC bridge balancing also depends on the harmonic distortion of the supply voltage [9]. An additional disadvantage may also be the reference of capacity, as this can be fairly substantial for high voltage.

2.3.4. Calorimeters

I previously mentioned calorimetric apparatus in the Motivation. When developing a new method, it is important to take into consideration its technical and economic feasibility. Not everything that is theoretically possible is realized. The biggest problems and disadvantages include:

- **Dimensions** – it would be impossible to transport the apparatus to the location of the machine that is to be measured. I would guess the apparatus could have a volume of approximately 40 cubic meters, maybe more. Moreover, it is necessary to transport the operating fluid and other auxiliary parts.
- **Insulation** – we mostly want to measure high voltage apparatus. It is necessary to ensure the proper connection and isolation of these apparatus.
- **Specificity** – it is not possible to dip all apparatus into a bath. The method has very low versatility.
- **Heat transfer problems** – continuous stirring is necessary. Heat transfer must be as even as possible.
- **Tardiness** – the measurement of large apparatus can take hours.
- **Price**

3. Two-stage transformers

The measurement of losses at low power factors requires very accurate transducers of voltage and current. The uncertainty of these instruments is usually described by a ratio error and a phase angle error. For measurement at low power factors, it is important to use a transducer with a minimal phase angle error. The phase angle error of ordinary instrument transformers or shuts is too large. The use of shuts is also limited by the maximum allowed dissipation. Some of the voltage dividers have very good parameters, but their use is associated with additional problems, particularly with galvanic isolation. Also, optical transducers may have a lot of potential, but they are still devices for the future. For these measurements, two-stage transformers have been developed. They are very important for measurements at low power factors and are not so well known; hence, I think it is worthwhile taking the time to describe them in detail.

3.1. Problems of ordinary instrument transformers

The principle of the two-stage transformer is to suppress the shortcomings of classic instrument transformers. Sources of uncertainty of ordinary instrument transformers include [12, 13]:

3.1.1. Magnetizing current

The magnetizing current is the main source of error for the vast majority of instrument transformers. We are trying to minimize this problem, but some current must flow in order to produce magnetic flux, which is essential.

3.1.2. Core losses

The primary current does not only produce a magnetizing current, it must also supply losses in the core. Magnetic materials with minimal losses should be used to suppress the ratio error which is most affected by core losses.

3.1.3. Flux leakage

A part of the magnetic flux does not link all the turns. This causes nonlinearity – the secondary voltage is not directly proportional to the primary voltage. It is important to maximize the core permeability, properly arrange the windings and use toroidal cores.

3.1.4. Impedances of windings

The error caused by voltage drops on the impedances is related to the magnetizing and burden current. The only solution is to use high-conductivity wires.

3.1.5. Insulation leakage currents

Due to the limited resistivity of winding isolation, there is a leakage current in the primary winding. It can be successfully suppressed by dividing the primary winding into sections. Constructional details are described in [12].

3.1.6. Stray capacitances

The stray capacitances of windings are not substantial because they are small, but it is very difficult to minimize them.

3.1.7. Capacitance between windings

Capacitance between windings can be relatively easily suppressed by an electrostatic shield.

3.1.8. Temperature dependence

As previous sources of uncertainty are much greater, the temperature dependence of conventional current transformers is negligible.

It is worth noting that for a conventinal insturement transformer that operates at 50 Hz, a substantial error is caused by the magnetizing current. Other causes of errors have little impact or are significant at higher frequencies. This is especially true for capacitances. I have mentioned temperature dependence here as we will work with it in later subchapters about two-stage transformers.

3.2. Equivalent circuit

According to [13], it is possible to draw a transformer equivalent circuit with the stray capacitances of the windings. The capacitance between windings is also mentioned, but most instrument transformers have an electrostatic shield. I have not mentioned the primary insulation leakage current, which should be presented as conductance, as it is difficult to express in this circuit.

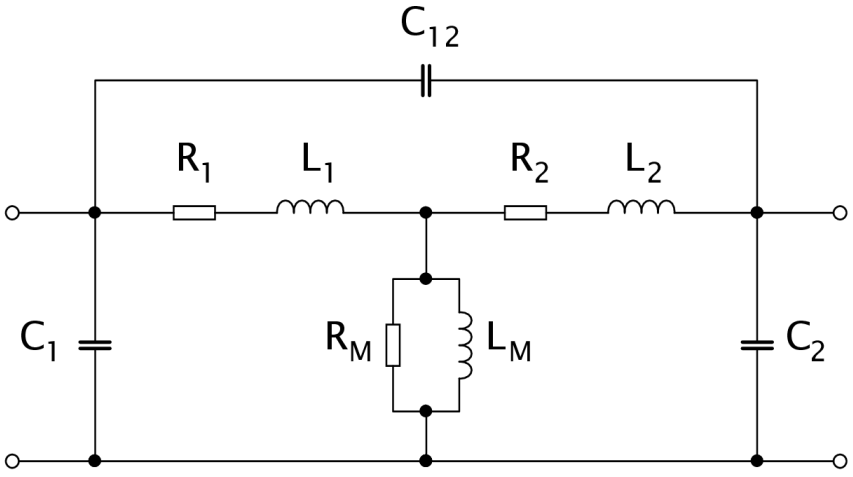

Figure 7. Transformer equivalent circuit

Where:

- R_1, L_1 and R_2, L_2 are impedances of windings
- R_M, L_M represent the magnetic circuit
- C_1, C_2 are stray capacitances and C_{12} is the capacitance between windings

3.3. Errors and their expression

The errors of conventional and two-stage transformers are expressed differently. While the conventional instrument transformer is described by the ratio and phase angle error, the error of two stage transformer is sometimes expressed by a fractional error.

3.3.1. Ratio error

The ratio error of the instrument transformer is defined by following formula:

$$\varepsilon_X = \frac{X_2 k_X - X_1}{X_1} \tag{17}$$

Where k_X is the ratio of voltage or the current transformer:

$$k_U = \frac{U_{1n}}{U_{2n}} \; ; \qquad k_I = \frac{I_{1n}}{I_{2n}} \tag{18}$$

X stands for voltage resp. current. The ratio error for a conventional instrument transformer is usually expressed as a percentage, whereas for a two-stage transformer it is expressed in parts per million and is sometimes called a quadrature error.

3.3.2. Phase angle error

A phase angle error or phase error is the angle between the primary current and the desired current $I_{1D,}$ which is 180 degrees away from the secondary current. This is illustrated graphically in Figure 8. For conventional transformers is phase angle error expressed in minutes. For older types of two-stage transformers it is expressed in seconds of arc, but for electronic compensated two-stage transformers it is expressed in parts per million.

3.3.3. Fractional error

A fractional error includes both the ratio and phase angle error. It is a complex number given in parts per million:

$$e = p + jq \tag{19}$$

It is not used for conventional instrument transformers and its use for two-stage transformer depends on the method that has been verified for accuracy. It is represented in the following equations [15]:

$$\frac{U_{2n}}{U_{1n}} = \frac{1}{k_U}(1 + e_U) \; ; \qquad \frac{I_{2n}}{I_{1n}} = \frac{1}{k_I}(1 + e_I) \tag{20}$$

In the following section I will write about two-stage current transformers as voltage transformers have better parameters, especially with regard to phase angle. I think, in principle, it is sufficient to describe one of them in detail; however, they are both very similar.

3.4. Phasor diagram of current transformer

If we neglect the primary leakage current and all capacitances, it is possible to draw a phasor diagram in Figure 8. Firstly, on the real axis, there is the magnetic flux and the magnetizing current which produces it. The electromotive force of the secondary winding lags behind the magnetic flux, according to Faraday's law of induction. In usual cases when the burden is a combination of the resistance and inductance, the secondary electromotive force leads the secondary current. For an ideal transformer, the primary current is 180 degrees away from secondary current, as the secondary ampere-turns are compensating for the primary ampere-turns, and there is no need for a magnetizing current or for supply losses. For a real transformer, however, it is necessary to generate magnetic flux in the core and this core has losses. These losses represent phasor $I_{1Fe,}$ which is inherently parallel to the electromotive force. The resulting required current I_{10} is given by the vector addition of these phasors. Lastly, the real primary current can be expressed from the desired primary current I_{1D} and supply current I_{10}. At first glance it is obvious that current I_1 is longer than the desired current I_{1D}. As a result, the measured value is smaller than it should be. In practice, this is corrected by reducing the number of turns of the secondary winding. However, at any rate, the phase angle error β remains [11, 14].

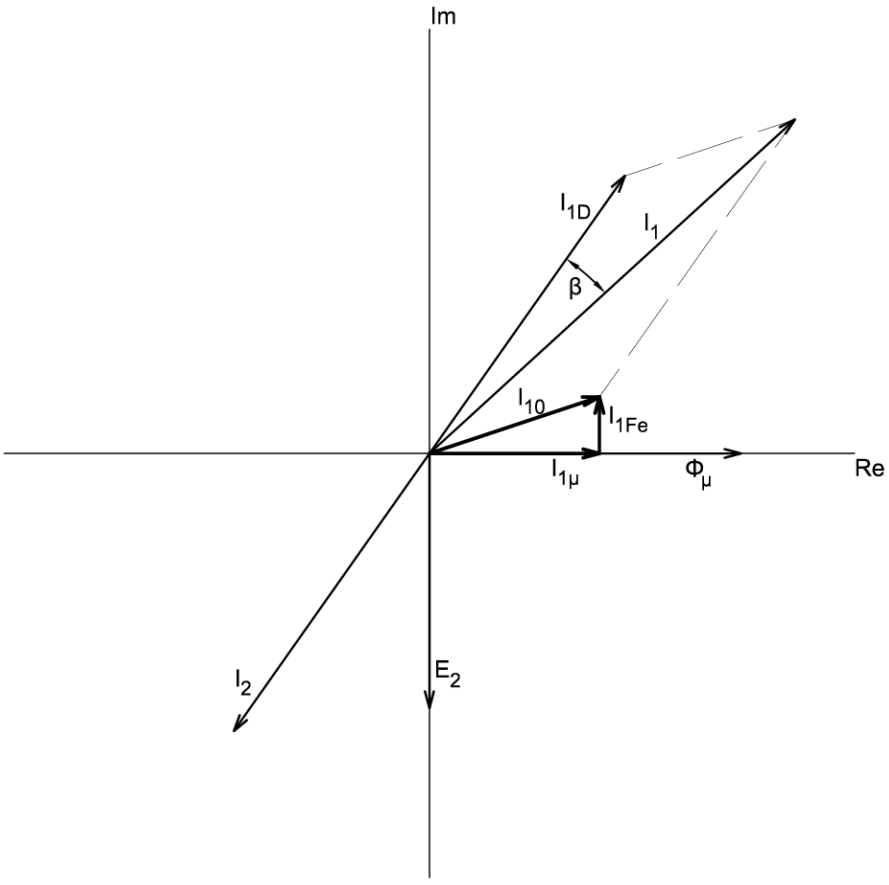

Figure 8. Phasor diagram of current transformer

3.5. Principle of two-stage transformer

The two-stage transformer is a surprisingly old invention. It is basically a precision instrument transformer with error compensation. The aim is to be as close as possible to an ideal instrument transformer. The compensation is realized by an electronic circuit that is connected to the secondary and special auxiliary winding. However, older two-stage transformers were based on analog compensation. The construction of this type of two-stage transformer is described in [11]. Principally, it can be expressed as two transformers. One of them is operating as an ordinary transformer and the other one is auxiliary, which helps to compensate for the ratio and phase angle error.

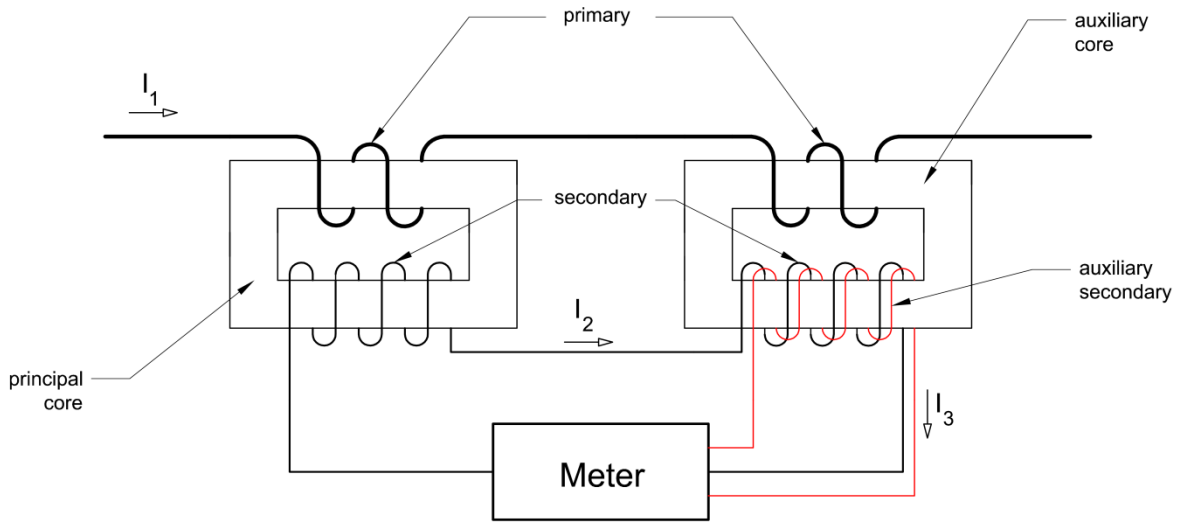

Figure 9. Schematic diagram of two-stage transformer

In the previous subchapter I mentioned that the supply current, which supplies core losses and produces magnetic flux in the core, is the biggest source of uncertainty. Unfortunately, the output of ordinary current transformers is the secondary current only. We know nothing about the magnitude or phase angle of the supply current I_{10}, and, therefore, it is impossible to refine the current I_1.

Two-stage transformers are based on knowledge of the supply current I_{10}. The auxiliary core performs the vector subtraction of the primary and secondary ampere-turns. They are of different sizes and between them there is a nonzero angle; therefore, magnetic flux in the core will be produced. This resulting magnetic flux is proportional to current I_{10} and since the auxiliary core is provided with additional winding, current I_3 is induced. This current is very similar to the supply current I_{10} of the first transformer, but unfortunately not quite the same because of losses and the magnetizing current of the auxiliary core. Current I_3 leads supply current I_{10} by a certain angle and there is also a small difference in magnitude, which is shown in Figure 10. Finally, if this current is vectorially added to the desired current I_{1D}, we obtain a compensated primary current which is much closer to the original primary current in magnitude and phase compared to current I_{1D}.

In practice, it is more convenient to realize the single primary and single secondary windings which are wound around both cores. However, the auxiliary winding is on the auxiliary core only. A two-stage transformer of this construction is more compact and its use in combination with a wattmeter or electricity meter is simpler.

As shown in Figure 10. the total error of an analog current two-stage transformer is much smaller than a conventional CT. The source of uncertainty is the inaccuracy of the measurement of supply current I_{10}. Nevertheless, the ratio error is between 500 - 100 ppm, and the phase angle error is smaller than two seconds of arc [11].

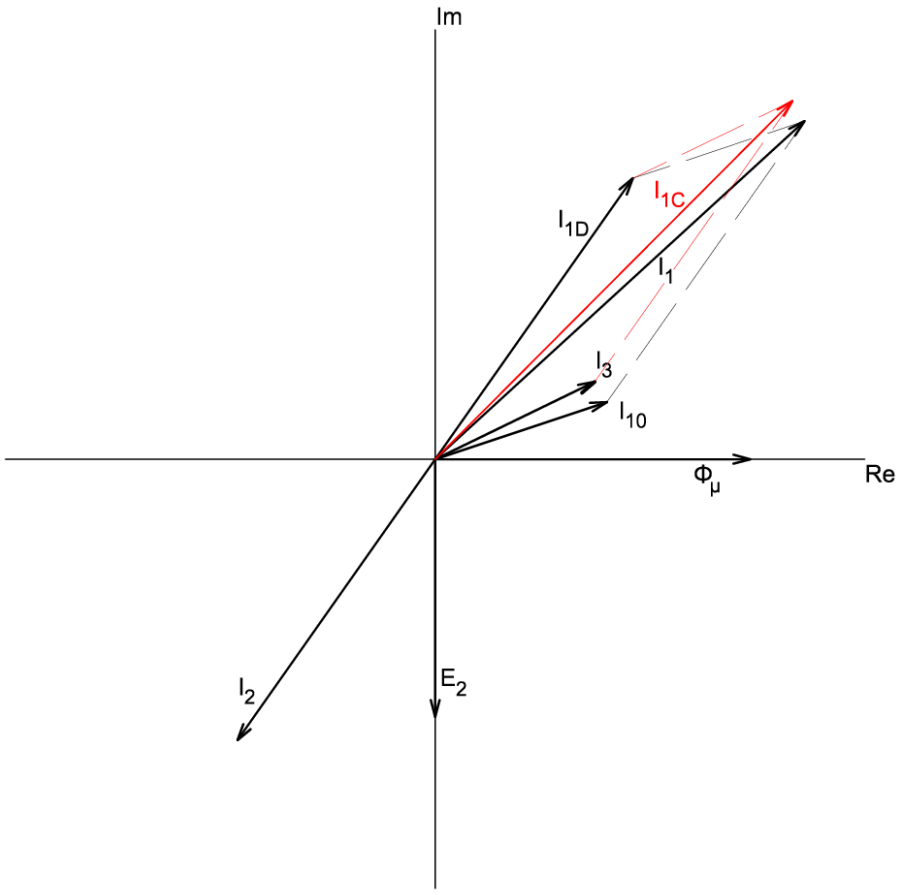

Figure 10. Phasor diagram of two-stage transformer

3.6. Two-stage transformer with electronic compensation

The principle of electronic compensation is based on the properties of the analog two-stage transformer. Therefore, I will build on the previous subchapter. Inherently, the current I_3 flows only if there is a difference between the primary and secondary ampere-turns. If this current is zero, the voltage in the auxiliary winding V_A is also zero, and vice versa. If we force the voltage V_A to zero via an external electronic circuit, no current will flow and the supply current I_{10} will be completely suppressed. In this case, the primary current will be identical to the desired current I_{1D} and we will obtain a phasor diagram of an ideal current transformer. At first glance, it looks as though the measurement is free of error, but, of course, there are other sources of uncertainty. However, none of these other factors cause as large an error as the current I_{10}.

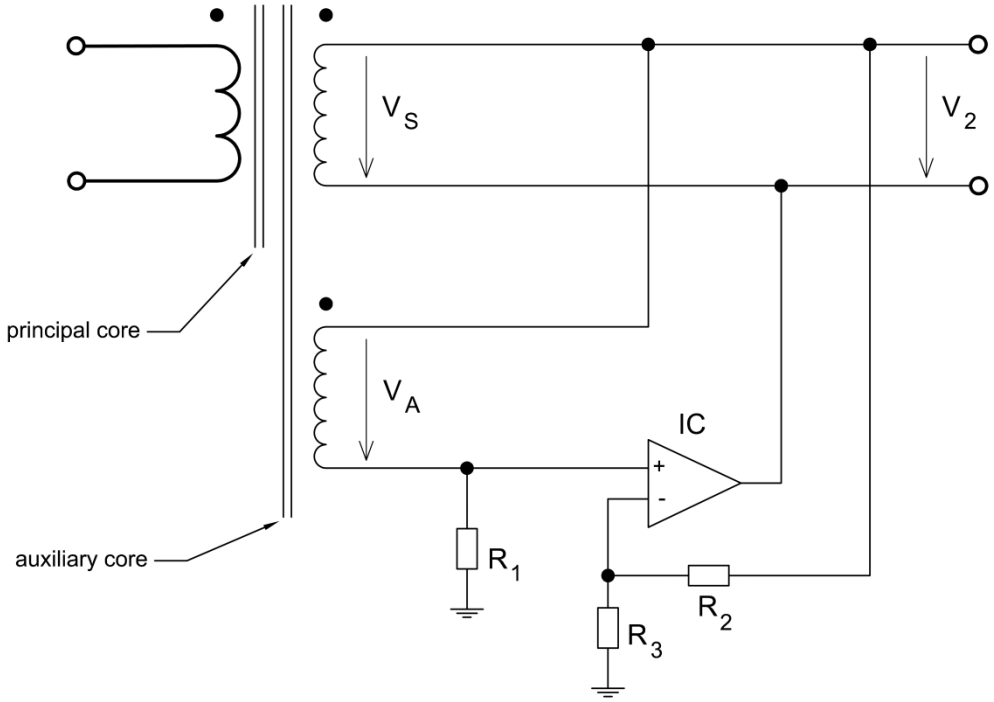

Figure 11. Two-stage transformer with electronic compensation

The operating principle of electronic compensation is as follows. Only a small amount of power is required to supply the auxiliary winding, so IC may represent a single operational amplifier and eventually an operational amplifier with boosting transistors on an output. The operational amplifier operates as a controlled voltage source and generates a voltage with opposite polarity compared to the voltage drop on the auxiliary winding. The following equations apply [13]:

$$V_A = (R_A + R_1)I + V_2 \tag{21}$$

which leads to [13]:

$$V_A = I\left(R_A + \frac{R_1 R_2}{R_3}\right) \tag{22}$$

3.6.1. Error sources

Resistors R_1 to R_3 may be very stable, but the auxiliary winding is made from copper and its resistance R_A varies at around 0.4 %/K. Therefore, the equation (13) is affected by temperature. This is the first source of error.

Another error is caused by capacitances. The capacitance between windings can be eliminated by an electrostatic shield that is grounded to an external grounding terminal, but the capacitances between this shield and the windings remain. Although it can be suppressed by shielded cables, this demands more space [16]. The influence of stray capacitances can be reduced by electronic compensation, although not entirely.

Another problem is associated with flux leakage. An equalization winding and magnetic shields are used to force the flux to be homogenous. More details are shown in [13], where a prototype of a current two-stage transformer is described.

3.6.2. Use of two-stage transformers and their limits

Accurate transducers are required for high precision measurements such as the calibrations of other measuring instruments, measurements at a very low power factor, and for accurate laboratory measurements. Two-stage transformers are the best choice because, besides their high accuracy, they have all the advantages of conventional instrument transformers. Nonetheless, conventional instrument transformers have higher maximum parameters and are cheaper.

The maximum voltage of two-stage voltage transformers is approximately 110 kV due to insulation and manufacturing limitations. The price of these transformers increases with increasing voltage. Two-stage transformer at 110 kV will be very expensive. Ordinary two-stage transformers have lower maximum primary voltages [17].

Two-stage current transformers may measure a current of about 1 kA at 350 kV. In the article ‘Optically Isolated Hybrid Two-Stage Current Transformer for Measurements at High Voltage’ [18] a hybrid two-stage transformer is described which is composed of two two-stage transformers in a cascade. Each of them has a current ratio of 1000/1 and an electronic compensation circuit is connected to the secondary winding of the second transformer [18].

Excellent accuracy can be achieved by a single two-stage transformer with electronic compensation. A two-stage voltage transformer with a fractional error (0 + 2j) ppm is described in [12]. Moreover, two-stage transformers are usually able to work at up to 10 kHz without an increase in significant errors [13]. Two-stage transformers with higher parameters are less accurate, especially two-stage current transformers with a cascade connection. These transformers have a ratio error of 70 ppm and a phase angle error of 25 ppm. In addition, their accuracy varies more with a measured current [18]. Two-stage voltage transformers for higher voltages are more accurate; their errors are approximately 3 ppm in the ratio and in the phase [17].

4. Digital signal processing

4.1. Zero crossing detection

An important part of DSP, or the program for calculating active power (for the method described in subchapter 2.1.), is the zero crossing detection algorithm – in particular when the error of numerical integration does not have a decisive influence, as I will mention in the next subchapter.

4.1.1. Point algorithm

The first way to determine the period is to find samples which go from negative to positive (for rising edges) or from positive to negative for falling edges respectively. Naturally, it is possible to calculate the period from such examples by using a known sampling frequency. This first possibility is described in the article 'Implementation of Power Measurement System with Fourier Series and Zero Crossing Algorithm' [23]. I will briefly describe the proposed procedure.

If the sampling frequency is an integer multiple of the signal frequency, it is possible to calculate the signal frequency from the formula:

$$f = \frac{1}{nT_S} \tag{23}$$

Where n is the number of samples within a period and T_S is the sampling frequency period. Of course, in practice, the sampling frequency is not an integer multiple of the signal frequency. Therefore, n is not an integer value, and thus it is necessary to calculate it.

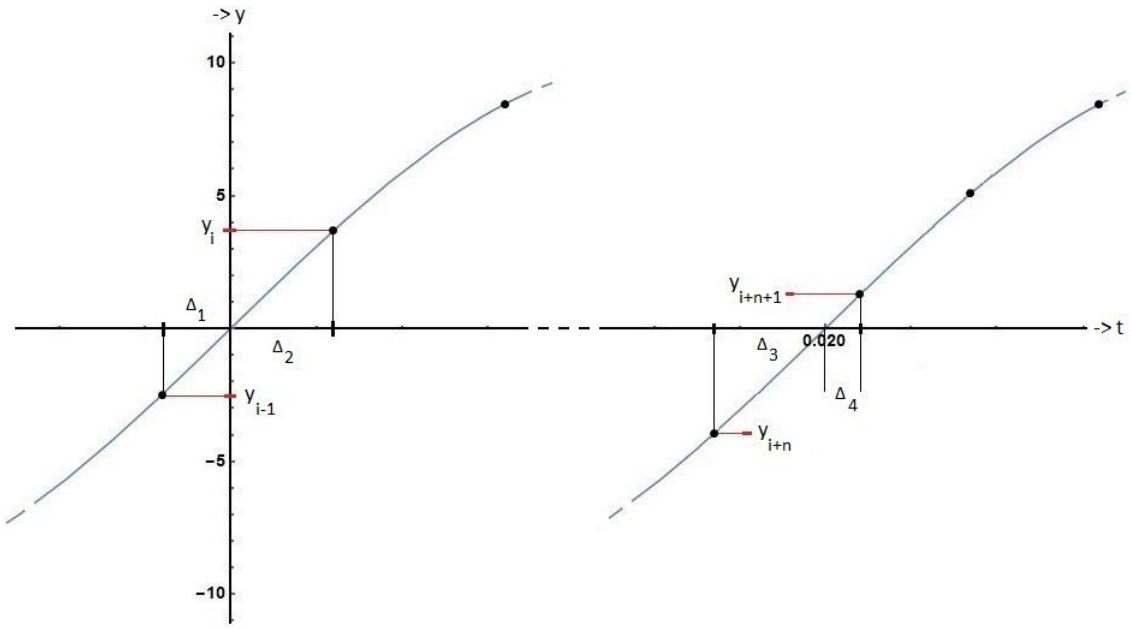

Figure 12. Zero crossing detection calculation

Two samples of densely sampled waveform can be joined by a line, in order to interpolate an accurate zero crossing point, as shown in the figure above. Using this procedure, we find the true value of samples within one period of the sampled signal, which is generally a non-integer number. The time distance between samples (black points) is equal to the period of the sampling frequency T_S. If we want to determine a period from the rising edges, we must look at two samples – the first of which is negative; the second of which is positive. We know the times in which these samples were taken, and, of course, their values y_{i-1}, y_i, y_{n+i}, y_{n+i+1}, (according to Figure 12.). Obviously, it is possible to express the following equations [23]:

$$\frac{\Delta_2}{\Delta_1 + \Delta_2} = \frac{|y_i|}{|y_i| + |y_{i-1}|} \tag{24}$$

$$\frac{\Delta_3}{\Delta_3 + \Delta_4} = \frac{|y_{i+n}|}{|y_{i+n}| + |y_{i+n+1}|} \tag{25}$$

Where $\Delta_1$to Δ_4 are the times between each intended sample and the point where the fitting line crosses the zero, which is actually the calculated zero crossing point. Equations (24) and (25) are corrections as actual n is a non-integer value. The actual value n_A is given by formula [23]:

$$n_A = n + \frac{|y_i|}{|y_i| + |y_{i-1}|} + \frac{|y_{i+n}|}{|y_{i+n}| + |y_{i+n+1}|} \tag{26}$$

Then, the actual frequency is:

$$f = \frac{1}{n_A T_S} = \frac{f_S}{n_A} \tag{27}$$

The presented method is very simple; its calculation is fast and it can be easily implemented for a digital signal processor (DSP). However, the method itself has many restrictions. It is not suitable for measuring waveforms that are distorted by strong noise as the calculation relies only on two samples that are also very small. Even so, the method gives very satisfactory results when it is supplemented by a discrete Fourier transform used as a filter [23].

4.1.2. Linear regression

The magnification of the sampling frequency corresponds with the increasing number of samples per period, and, importantly, it also corresponds with the sizes of samples near the zero crossing point. The higher the sampling frequency, the smaller the samples near the zero. For a signal with noise or for a signal with interpolated disturbances of another type, it is better not to rely only on two samples near zero, but to take more samples and use a fitting line to determine the actual zero crossing. Figure 15. shows a situation in

which the first method fails because one of the samples is very close to zero and is influenced by noise, and, therefore, has a different polarity. However, linear regression in this case determines the zero crossing point relatively accurately. The main challenge of linear regression is to estimate the appropriate number of samples which should be fitted.

There are other options for determining the period. For instance, the other method that I tested does not need the zero crossing detection. Nevertheless, zero-crossing detection is very often used. For instance, the power analyzer Yokogawa WT 3000 uses a zero crossing algorithm [26] that is unfortunately impossible to delineate because it is part of the know-how. I know this personally, because I spoke with a technical sales advisor during the preparation of my bachelor thesis.

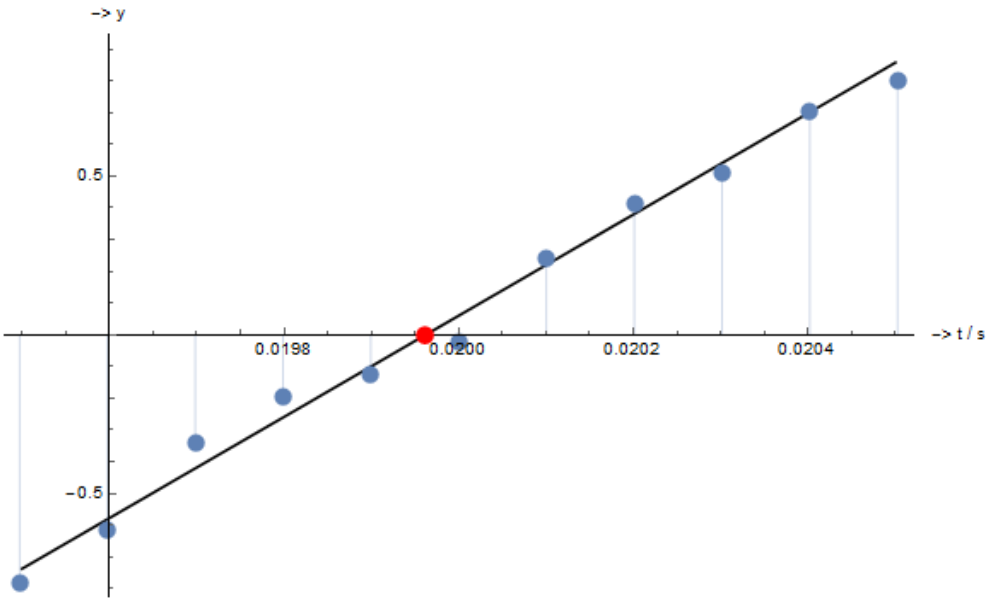

Figure 13. Linear regression

The red point indicates the zero crossing that was obtained by linear regression. The point algorithm failed in this case because the determined period will be shorter than the actual period.

In both these subchapters I used raising edges of waveforms, but of course it is also possible to use falling edges. To conclude, I would seem that there is no best method, since the accuracy of the zero crossing algorithm depends on many factors. In my opinion, the best solution is based on experience from real measurements.

4.2. Numerical integration

Numerical integration is an inseparable part of DSP. For the measurements discussed in this Diploma thesis, the right-hand rule or the left-hand rule are not appropriate methods, as they greatly overestimate or underestimate the real value. These methods may suffice in areas that depend on computing speed and in which accuracy is not a priority. Similar could be said about the midpoint rule (sometimes called the rectangle rule), which is more accurate but is not a good choice for the purpose of measurement. More sophisticated methods are required in the field of precision measurement. From my own experience, the trapezoid rule for densely sampled waveforms works very well. However, for a purely sampled signal it is appropriate to use Simpson's rule. Generally, the numerical integration formulas have the following form [27]:

$$\int_a^b f(x)dx \approx w_0 f(x_0) + w_1 f(x_1) + \ldots + w_n f(x_n) \tag{28}$$

This type of formula includes the midpoint rule, trapezoid rule, and Simpson's rule. In this formula, we can distinguish two sequences. The first is the sequence of sampling points $\vec{\mathrm{x}} = (\mathrm{x}_0, \mathrm{x}_1, \ldots, \mathrm{x}_\mathrm{n})$ and the second is the sequence of weights $\vec{w} = (w_0, w_1, \ldots, w_n)$. The sequence of sampling points is given by measurement, while the sequence of weights may vary with each rule. A more detailed analysis shows that the use of Simpson's rule is restricted by the number of points as it is necessary to ensure that an odd number of samples are used for the calculation. This is caused by weights, because for Simpson's rule there is always an odd number of weights. If we must use an even number of samples then it is necessary to remove one sample and to calculate an odd number of samples using Simpson's rule, and then calculate the rest using the trapezoid rule. Nevertheless, the accuracy of the trapezoid rule for densely sampled waveforms is comparable to Simpson's rule [27]; because of this, I will use it in the method for calculating the mean value over a period.

5. Testing model

5.1. Description of the model

In this part I will describe the model for testing methods as well as the program for testing the trapezoid method when the active power is calculated from more periods.

5.1.1. Comparison of methods

This program is in the Appendix D under the name of Appendix D - Comparison of methods.

1. At the start, auxiliary variables are defined, and the working directory is set to the notebook directory.

2. In the first part, the waveforms of voltage and current are defined, as well as the phase angle and auxiliary variable that is presenting the sampling frequency. Waveforms have a defined period and their multiple is integrated over this period to calculate the reference active power.

3. In the next part, the function for sampling and quantization is defined. The input parameters are (first things first): voltage, current, the number of samples, the maximum time of sampling, the range of the voltage converter, the range of the current converter, and the number of bits. The output is composed from the time, the quantized voltage and the quantized current.

4. From this point, the method based on phasor measurement begins. In the first part, windows are determined according to subchapter 2.2.3. Consequently, standard deviations are calculated and the three lowest standard deviations are selected.

5. The minimum is then calculated from these three deviations, from which the frequency or period is calculated respectively.

6. As the sampling frequency is generally not the integer multiple of the frequency of the observed signal, a correction is made here that recalculates the original number of the samples to one period.

7. The phasor is calculated using tables of sine and cosine functions. The resulting phasor is calculated according to equation (12).

8. Here, the inputs are recalculated if necessary and data can be viewed for inspection.

9. In this part, the maximum number of harmonic components is set. In this case, the value is set to 40, according to previous text. Tables of sine and cosine functions for higher harmonic components of the signal are also in this part.

10. Finally, the active power is calculated in accordance with equation (8).

11. In this part, the second method begins. The auxiliary variable is defined at the start and there it is also possible to set the hysteresis for zero crossing determination.

12. In the next part, the voltage input data is modified using the selected voltage hysteresis. This data is then split. After these adjustments, each zero crossing has its own data and it is possible to calculate the fitting line, and from it to calculate the zero crossing point. From these points it is then possible to calculate the voltage period.

13. This part is the same as the previous part, only here I am working with samples of current. The current period is calculated from the zero crossing points.

14. The instantaneous power is calculated in this part, as well as the period that I determined as the arithmetic mean of the voltage and current period. Using For cycles, the first and the last sample are selected for calculating the active power by the trapezoid rule.

15. Finally, the active power is a result of the trapezoid rule. In this part, the absolute value of active power error is also calculated, which is in Watts.

16. The absolute error is then recalculated to a relative error as a percentage, and the values are expressed by several graphs.

5.1.2. Trapezoid method using averaging

This program is in the Appendix E under the name of Appendix E – Trapezoid method using averaging. The program is quite similar, so I will often refer to the previous subchapter.

1. The first part is the same as parts 2 and 3 of previous subchapter.

2. In the second part, the voltage and current waveforms are modified similarly as in 11, and the zero crossings points are calculated as in parts 12 and 13.

3. Instantaneous power samples are calculated, as well as the times which corespond with one, ten and one hundred periods. Suitable initial and final samples are again found using For cycles, and the instantaneous power is then integrated using the trapezoid rule for each considered number of periods.

4. The absolute value of active power error is recalculated to the relative error and presented in similar graphs.

5.2. Simulation results

5.2.1. General comparison of methods

The following figure shows the dependence of active power error on the phase angle. The blue points represent errors when trapezoid integration is used and the period is calculated from zero crossings, which are determined by linear regression. The red points represent errors when the calculation based on the phasor measurements is used. This chart is good for basic understanding, but for closer examination it is better to express dependences on the logarithmic scale.

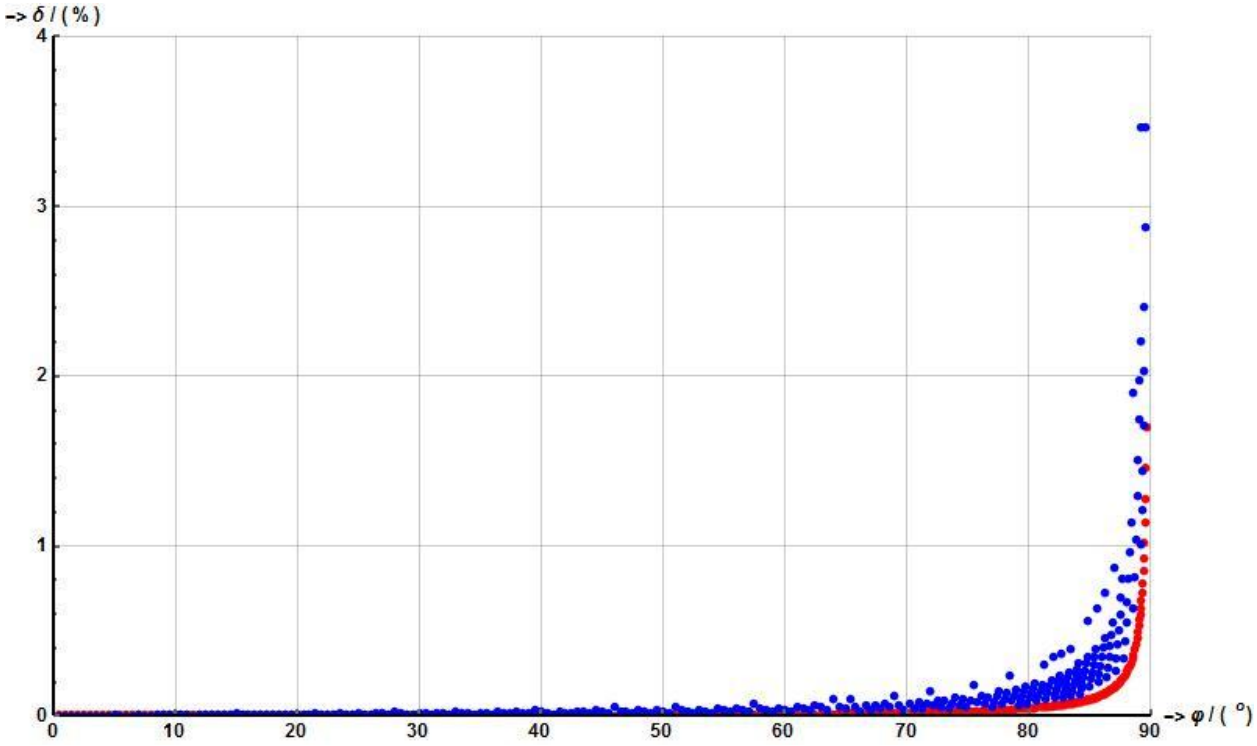

Figure 14. General comparison

Test conditions were as follows:

- Harmonic waveforms (V = 100V and I = 5A).
- A/D converters' ranges are 150V and 10A and both have 12-bit resolution.
- Sampling frequency is 25 kHz and the frequency of the sampled signal is 50 Hz.

For a better comparison it is appropriate to choose some comparative criterion. The fact that dependences are composed of discrete points makes this assessment even more difficult. If we want to assess the entire interval, which is expressed in these particular charts, then I think there is no better solution than to calculate the error arithmetic mean. The first chart is very clear. The method based on trapezoid integration has a greater error and both methods have a greater error for lower power factors, as was expected. However, the logarithmic scale, which is used on the next chart, allows a better view.

From the next following it is evident that the resulting dependence is not so clear because the trapezoid method is more accurate for a phase angle lower than 20^{o} (approximately). Even so, if we consider the whole range, the method based on phasors measurement is better.

The error arithmetic mean of the trapezoid method (in the range $\varphi = 0.5^{o} - 89.7^{o}$) is 0.267 %, while the error arithmetic mean of method based on the phasors measurement is 0.093 %. If we only consider the measurements at the low power factor, the difference will be even greater. This is clearly shown in the chart on the next page where the inverse logarithmic scale for phase angle is used in order to emphasize values at the low power factor.

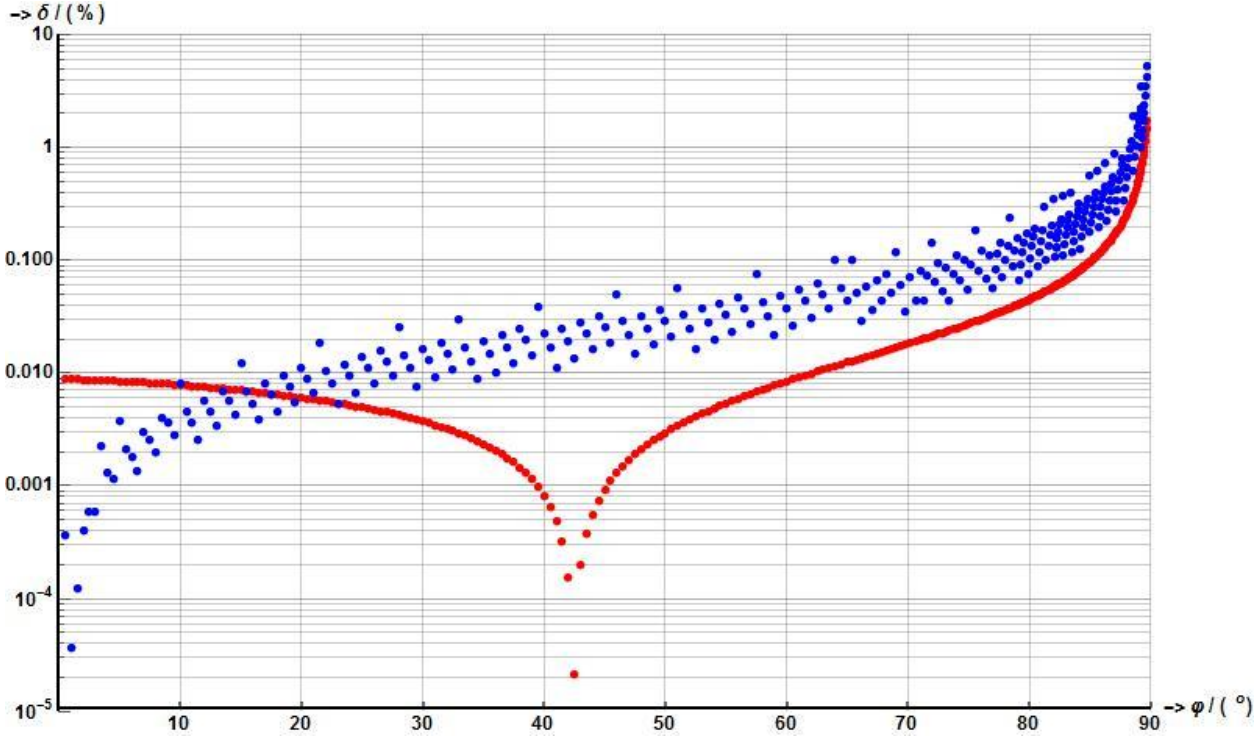

Figure 15. General comparison - logarithmic scale

The error's trend of the trapezoid method corresponds to the previous results in [19]. Only the error is greater as in this case it is also an error of period determination. The values of each calculation are slightly different as it depends on the error of the trapezoid method and also on the error of period determination. This method has achieved the best results for power factors approaching one, but that is not an area in which we are interested.

Regarding the second method, the first interesting thing is that there is a certain area where the error is very small. In this example, the error in this area is around 0.2 to 90 ppm. I have been thinking about it, but I know nothing further except that it depends on the sampling frequency, or on the ratio of the sampling frequency, and the frequency of the sampled signal. Nevertheless, it is not essential to look for the cause of the error. In my opinion, in practice measurements, it would be impossible to detect this small difference as even the most accurate instruments have an error of about several ppm for voltage measurements, and current measurements are usually less accurate.

Naturally, power measurement is burdened with even bigger error as it is a combination of both these measurements. I have already mentioned this dependence in subchapter 2.1.1.

The following graph highlights the area with a low power factor. It is evident that the active power error is growing rapidly, and for small power factors it is many times greater than for pure resistive load. The difference between methods is greater for the smallest considered power factor (for the biggest phase angle). This difference varies according to the phase angle as the method based on trapezoid integration has a large dispersion of error values. For small power factors (a phase angle of approximately 85°) the error of the second method is about 0.1 % while the error of the first method is between 0.2 – 0.5%. This corresponds to the power factor of 0.087, which is typical value for small reactors. For large reactors and capacitors, the power factor is even smaller – a typical value is 0.002. The phase angle in this case is approximately 89.9°. The difference between methods is more significant – while the method based on the phasors measurement has error of between 0.6 – 1.8%, the method based on trapezoid integration has error between 1-5%.

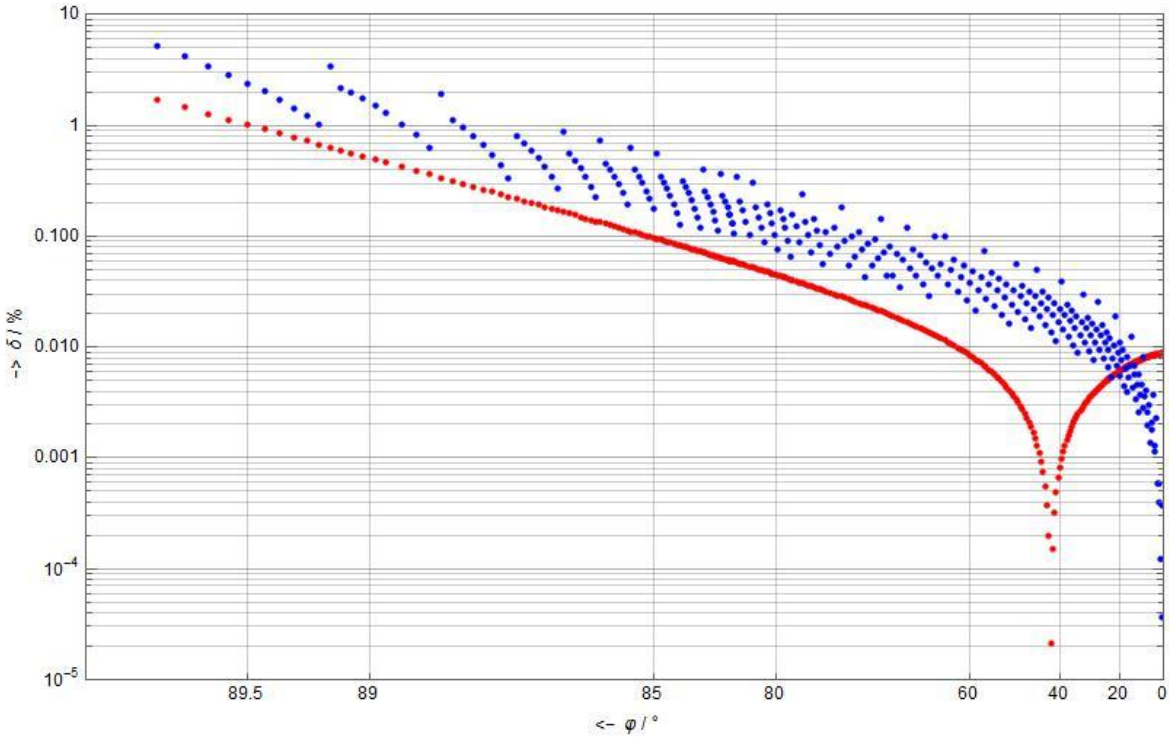

Figure 16. General comparison - inverse logarithmic scale

The theoretical model indicates that the elimination of zero-crossing detection is justified because it leads to greater accuracy of power measurement at low power factor. Moreover, in this thesis I have used linear regression for the determination of periods, which is unlikely to be used in digital processors of power analyzers because of its computational complexity. The second method, which is based on phasors measurement, is designed to be programmed to a processor, so the question is which algorithm is used in power analyzers to determine the period. In any case, zero crossing determination is not recommendable, and it depends on whether or not it is worth changing the existing algorithms.

5.2.2. Trapezoid method using averaging

One ways of refining the power measurement is to measure the active power from more periods. Similar to period measurement, it is possible to use averaging to calculate active power from more periods. While the error in time determination is constant, the measured time might be longer, thus the error in time determination will be less significant. The following figure shows active power error when the power measurement is realized from one period (red points), ten periods (blue points) and one hundred periods (green points). The average error when the active power is calculated from one period is 0.242%, while the average error for calculations from ten periods is 0.024 %, and for calculations based on one hundred periods is 0.00245%. So theoretically, the power measurement is n-times more accurate, where the n is the number of periods considered in the calculation. This is true, of course, under certain circumstances. For instance, during the measurement changes may occur in the parameters of the measured instrument, or a change in supply or other disturbance that can be difficult to predict. In that case, the shorter measurement is better. These two thinks go against each other, so it is important to find a reasonable compromise.

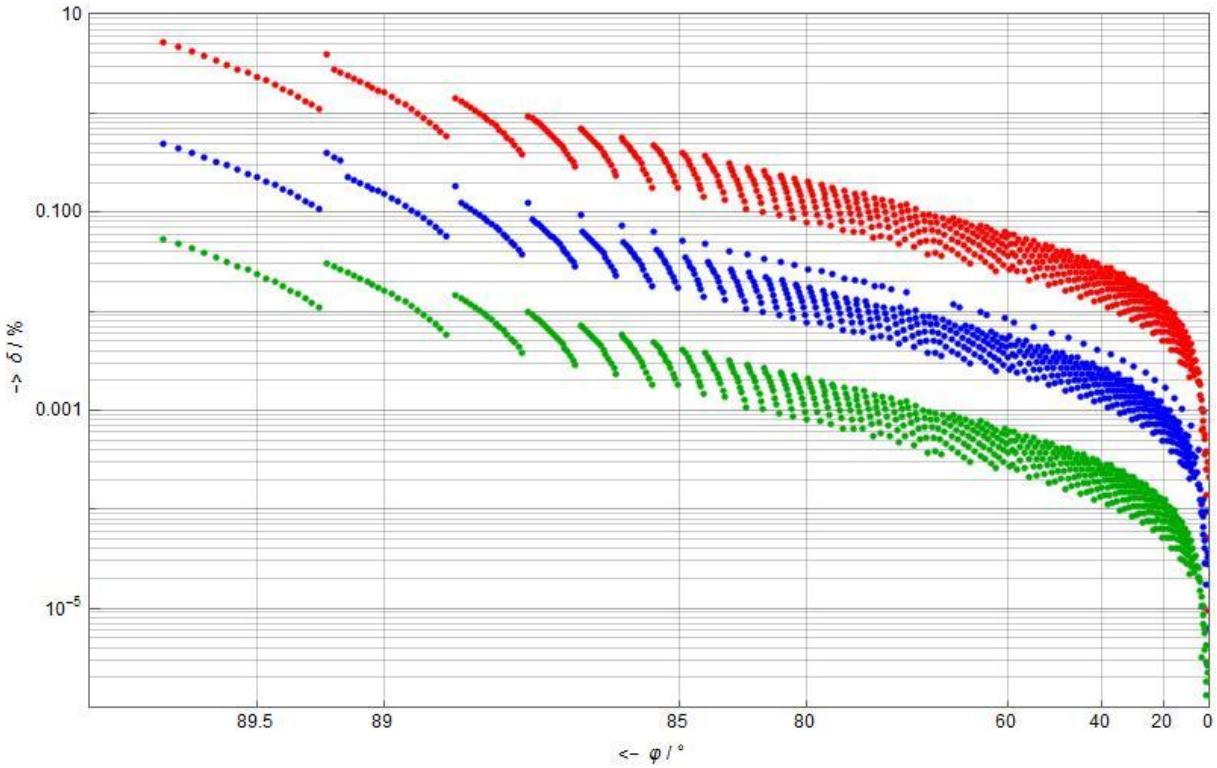

Figure 17. Trapezoid method using averaging

6. Power measurement system

I mentioned various types of loss measurement in the second chapter. Some of them are universal as it does not matter if the measured load is capacitive or inductive. It is the first feature that must be met in the power measurement system, along with other requirements. Using the previous chapter about two-stage transformers, which solved the problem with transducers, it is possible to design the following schematic diagram for active power measurement at a low power factor.

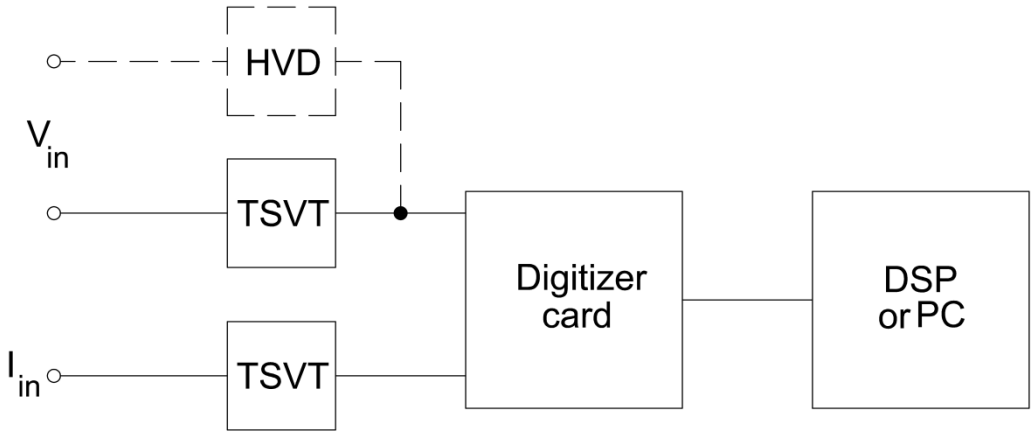

Figure 18. Power measurement system

Where HVD is a high voltage divider that can be used instead of a two-stage voltage transformer (TSVT); however, it is then necessary to ensure galvanic isolation. Current measuring requires a two-stage current transformer (TSCT) – there is no alternative option. These voltage and current transducers must have an output suitable for a digitizer card, which is not a problem for two-stage transformers because their outputs are different from conventional instrument transformers. Both of them might have an output of a few volts, but for other types (especially for 110 kV two-stage voltage transformers or HVD), it is necessary to use an additional divider, which is not mentioned. This additional divider must be as precise as other parts of the measuring chain, although it is not critical as it may be designed only for low voltage. The digitizer card is an ultra-fast waveform digitizer card for PCI bus [25] that takes care of the waveforms discretization. The resulting data can be processed on a PC or in a digital signal processor with a specific interface. In the following subchapters, I will focus on individual parts of the measuring chain and the problems associated with them. This will also be a launch pad for our real measurements in a high-voltage laboratory.

6.1. Digitizer card

The digitizer card is a key part of the proposed power measurement system. I will focus on the digitizer card CompuScope 1610 and 12100, both of which are in the laboratory and both of which I used. In short, these cards are high dynamic performance digitizers for precision measurements, which means measurement at low power factors. They are produced by Acquitek Company, which is a specialist in data acquisition systems.

The CompuScope 1610 has two channels that allow two analog signals to be simultaneously sampled by a selected speed. Both channels have 16 bit resolution, which for a card of this type is one of the best values on the market. Figure 19. shows a simplified block diagram. Coupling capacitors and a bypass switch are seen on the input of each channel and also on the input of the external trigger. Signals from the input channels are yielded to the operational amplifier, which has external offset resetting. Other circuits then ensure that the signals are taken at precisely the same time – this is important for many applications, and is absolutely necessary for power measurements based on the calculation of the mean value of the instantaneous power. The dashed line indicates the border of the analog and digital part and also refers to the two-board configuration. It is appropriate to isolate the high-frequency analog circuitry from the bus-related digital electronics due to digital noise [25].

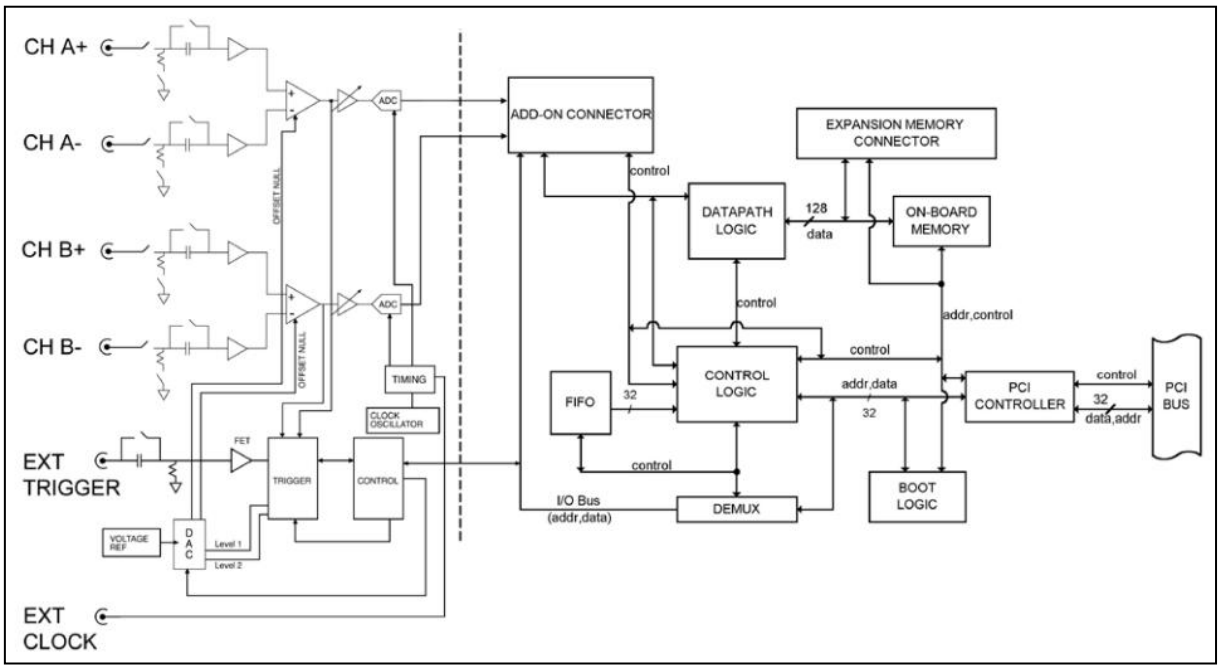

Figure 19. CompuScope 1610 Simplified Block Diagram

However, during my practical measurements, we found that there are interpolated strong disturbances on channel A of this card, which were suspiciously periodic. After excluding other causes, we came to the conclusion that there is a problem in channel A of this card. It looks like an AD converter has been damaged as the values of some samples are greater than they should be, and this shift is the same for all of them. Therefore, I used digitizer card CompuScope 12100 for my other measurements. However, CompuScope 1610 is preferable as it has higher voltage inputs and higher bit resolution (see Appendix A).

The parameters of CompuScope 12100 are listed in Appendix B. Generally, we can say that this card is not as suitable as the previous one. It has a higher sampling rate but also a lower bit resolution. As I mentioned in the subchapter about active power error, the bit resolution of converters is more important than the sampling frequency. Nevertheless, the bigger restriction is that this card has a lower input voltage, which requires the use of a transducer with a higher ratio. Unlike the previous card, the CompuScope 12100 digitizer card does not have differential inputs. However, their input circuitry is very similar. The card has two channels with 12-bit nominal resolution.

6.2. Practical measurement performance

6.2.1. General description

Unfortunately, at the university laboratory, we have no two-stage transformers. As I described in previous chapters, without the current two-stage transformer it is not possible to measure with high accuracy. One option is to use a transducer with an exactly known error, and then to correct the final value. The other option is to measure at lower voltages where we do not need any transducer and where is a sufficient low voltage input of digitizer card. It is not applicable for practical measurements, but it is a simplification that we have to do.

During practical measurements I measured two different reactors and also tried to determine the losses of the film capacitor. After several attempts, I found out that film capacitors could not be measured at low voltage because the current flowing through the circuit is too small. Measurement on reactors appeared perspective, but we failed to find an accurate reference measurement that would allow a better method to be determined. I put great hopes in the measurement of air coil because it is possible to determine DC resistance with high accuracy, and skin effect can be neglected. However, air coils have big resistance while their inductance is small, so the resulting loss angle is great. The graphs in the previous chapter show that the difference between the methods for big power factor is very small. Actually, it is practically under uncertainty of practical measurements. Another possibility is to measure losses by an accurate bridge, but even this procedure has significant shortcomings. Firstly, the bridge measurement is realized on a single frequency, while the actual measurement is distorted by higher harmonics. And more importantly, the difference between methods is smaller than the uncertainty of the bridge that is in the laboratory [29]. The difference between methods is bigger for very small power factors, but in these cases the bridge balancing fails, and the resulting value is unreal. I will mention this problem about reference later as it will be clear how much the results differ.

6.2.2. Description of the scheme

As I mentioned, I measured the losses of two reactors, but in the first measurement it was necessary to use a transducer for voltage, due to the relatively high resistance of the winding of the reactor, so I am presenting the second measurement which was realized on the reactor which I borrowed from the Department of Electrical Drives and Traction. The label and photos of this reactor, as well as the photo of measuring workplace are in Appendix C.

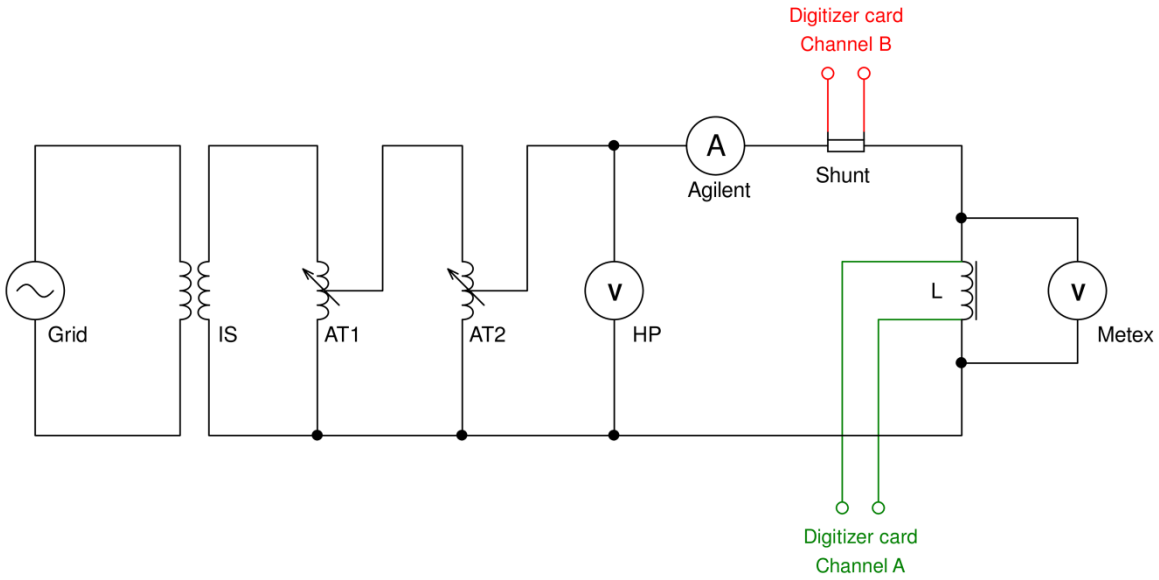

Figure 20. Measurement scheme

In order to isolate the measured reactor from PC it is necessary to use isolation transformer IS. It is possible either to isolate the PC with a monitor or to isolate the measuring circuit. Both variants are functional. Behind the isolation transformer are two autotransformers in a cascade that is appropriate, due to the low voltage input of the digitizer card and the small resistivity of the reactor winding. An Agilent multimeter measures the current through the circuit, and an HP multimeter measures the voltage on the output of the second autotransformer. Multimeter Metex serves to control the voltage at the card input. Voltage on the reactor is sensed directly from reactor terminals, while the current is sensed from the shunt. Using a shunt brings additional error, but out of the options that we have, it is the best.

6.3. Description of the program

The program for practical measurements is based on the program of the testing model, but there is also one notebook for data modification.

6.3.1. Program for input modifications

This program is in Appendix F under the name of Appendix F – Program for input modifications. Here is a brief description:

1. In the introductory part, the data is retrieved from the asc files.
2. Samples are split to time, voltage and current sequence and then down sampled to the desired sampling rate.
3. Modified data is exported to an xlsx file to three columns for time, voltage and current.

6.3.2. Computing program

The computing program uses the input data from the xlsx file, but most of its parts are the same as in the testing program. Only some conditions are changed, in order to secure flawless processing of real data. The program is in Appendix G.

1. In the first part, the input data are imported and auxiliary variables are defined.
2. The next part contains methods based on the phasors measurement. (Steps 4 – 10 from subchapter 5.1.1.).
3. This part is dedicated to the first method. The condition for splitting zero crossing data is slightly changed in order to separate data more reliably.
4. Output is presented in Watts for each method.

6.4. Results and evaluation of measurement

Photos of measured reactor and measuring workplace are in the Appendix C.

In the first calculation, I used sampling frequency 25 kHz because it is the same frequency that I used in the testing model. Bit resolution is also the same as in the testing model because the digitizer card has 12 bit resolution. The current, which flow through the reactor, was 1 A, and power factor was approximately 0.08. Results are as follows:

$$\mathbf{P_{AP25} = 0.4828\ W}$$

$$\mathbf{P_{PM25} = 0.4808\ W}$$

Index AP refers to the first method, which is based on the calculation of the average value of instantaneous power over a period while the index PM refers to the second method. The difference between results is approximately 2mW, which is an indistinguishable value in the practical measurements.

The error of the digitizer card depends on the range used, and for 5V range it is 1 % and for 2 V range it is 0.5 %. The resulting uncertainty is the uncertainty of indirect measurement, and surely it is greater than the larger one. The shunt used also has error, as well as the digitizer card has phase angle error, but these errors are negligible (in comparison with the error of the digitalizer). However, calculations are performed from the same data, so this difference is not the result of uncertainties in measuring circuitry. I just want to point out that the difference between these two methods is practically negligible. Real measurements depend mainly on the accuracy of the measuring devices used, not on the method of data processing.

In other calculations, the difference is greater. Here are the values for 50 kHz sampling frequency:

$$\mathbf{P_{AP50} = 0.4831\ W}$$

$$\mathbf{P_{PM50} = 0.4801\ W}$$

Nevertheless, even in this case it is not possible to say which method is better, because other measurement like bridge methods will fail to determine the component of active power, which is created by higher harmonics, and the difference is also very small. It is interesting that the results are almost the same. Active power calculated as the mean value over a period is, again, a little bit greater. Values for 100 kHz sampling frequency are as follows:

$$\mathbf{P_{AP100} = 0.4832\ W}$$

$$\mathbf{P_{PM100} = 0.48\ W}$$

And because I mentioned the possibility to calculate active power from more periods, I am also presenting the active power calculated from four periods at sampling frequency 25 kHz:

$$\mathbf{P_{4AP25} = 0.4843\ W}$$

Calculations can be summarized as follows. Active power based on the phasor measurements is between 0.48 – 0.4808 W, while the active power calculated by the first method is between 0.4828 – 0.4832 W. Active power calculated from more periods is a little bit bigger than the calculation from one period. The difference between methods is approximately 3mW, and this difference is almost independent on the sampling frequency.

It would be great to say which method is more accurate, but it is not as easy as it looks. Active power calculated as the average value over a period from instantaneous power samples is a little bit greater than the active power that was calculated from phasors. Nevertheless, the problem of realization of normal of active power (or normal of losses) is critical. The realization of active power reference in which the resistive component dominates is not the same challenge as the realization of this reference with a large reactive component. I measured the resistivity of air coil winding with an expanded uncertainty of 7 mΩ, and the winding had 3.193 Ω. If the other multimeter, which has an excellent accuracy, were available, it would be possible to reduce the uncertainty even more. However, these measurements are pointless because the biggest difference between methods is at low power factors. The phase angle of air coils is around 10 – 20^{o} due to its large resistive component. Moreover, it is certainly not an area measuring losses at low power factors. A suitable power factor for loss measurement has capacitors and coils with a ferromagnetic core. In principle, both of these devices have component of losses that is different at AC current. For instance, the DC resistivity of one reactor that I measured was 8 Ω, but the AC resistivity (which includes the core losses) was 11.1 Ω. I did not measure capacitors, but it is the same problem, and in addition, there are other problems with measurement (the current through a circuit is hardly measurable if the measurement is not realized at high voltage or for a capacitor with big capacity).

After finding that an air coil is not a suitable reference, I thought that the bridge method might help. Unfortunately, because of reasons that I have already mentioned in subchapter 6.2.1, it is not possible.

The difference between methods is approximately 3 mV, which is not critical, but it seems that a comparison of methods in practice will require further, more accurate measurements. But from the results it is evident why the zero crossing algorithm is still used. For waveforms that do not pass the zero many times, and for which it is not difficult to find period, using zero crossing is fully sufficient for determining a period.

Overall, it would seem that software is not the main source of uncertainty, and better results can be worked out mainly by improving hardware. It does not change the fact that poor digital processing can spoil the result of each precision measurement.

7. Conclusion

The measurement of losses at low power factors has been discussed for a long time. Even nowadays it is an actual topic, especially due to power analyzers and digital signal processing in general. In this thesis, I followed the bachelor thesis, which helped me a lot because measurement at low power factors is quite a broad topic. At the beginning of this thesis, I mentioned measurement options and fundamental motivation for loss measurement. These introductory chapters are followed by a chapter on two-stage transformers, which is, I think, one of the most important parts of this thesis, even if it is just a theoretical description. I found this article by chance, but two-stage transformers are perfect instruments for high precision high voltage wattmeters. A certain part of the work is also dedicated to zero crossing algorithms because it is a leading technique in period determination for most devices, including power analyzers. The practical comparison of methods proved to be a tough task, and I have to admit that I am not very satisfied with the results myself. But according to me, even this failure means something. I think that an endeavor to improve computing software is not worth the effort because the predominant sources of uncertainty lie elsewhere. The difference between methods is greater than half a percent, which is quite a lot for an unexceptional power measurement at a normal power factor, but the difference is rather small for a measurement that was realized at power factor 0.08 (approximately).

More openly, I am glad that I can present this thesis in English. The work was much lengthier than in Czech because I had to learn many things, and I was also very careful with re-reading corrections because I know that when reading someone else's text in another language, it is easy to have misunderstandings. However, I enjoyed writing in English more than in Czech, so I think it was a good idea and great challenge as well.

References

[1] Czech Republic. Public notice No. 347/2000 Sb. In: Jihlava: ERO, 2012. Available from: http://www.eru.cz/en/-/vyhlaska-c-347-2012-sb-?inheritRedirect=true

[2] Moore, J.M., "A Technique for Calibrating Power Frequency Wattmeters at Very Low Power Factors," Instrumentation and Measurement, IEEE Transactions on , vol.23, no.4, pp.318,322, Dec. 1974, doi: 10.1109/TIM.1974.4314302

[3] Seguin, B.; Gosse, J-P; Sylvestre, A.; Fouassier, P.; Ferrieux, J-p, "Calorimetric apparatus for measurement of power losses in capacitors," Instrumentation and Measurement Technology Conference, 1998. IMTC/98. Conference Proceedings. IEEE , vol.1, no., pp.602,607 vol.1, 18-21 May 1998, doi: 10.1109/ IMTC.1998.679863

[4] Carroll, Joseph S.; Peterson, Thomas F.; Stray, George R., "Power Measurements at High Voltages and Low Power Factors," American Institute of Electrical Engineers, Transactionsofthe , vol.XLIII, no., pp.1130,1138, Jan. 1924

[5] Kyncl, J.; Hariram, A.; Novotny, M., "On measurement of synchronous phasors in electrical grids," Circuits and Systems (ISCAS), 2013 IEEE International Symposium on , vol., no., pp.2972,2975, 19-23 May 2013, doi: 10.1109/ISCAS.2013.6572503

[6] Zhang, Zhengkao. Digital technique for on-line measurement of dissipation factor of high voltage apparatus. University of Manitoba, 1997. Available from: http://www.techlib.cz/cs/. Master's thesis. Department of Electrical and Computer Engineering. Advisors: M. R. Raghuveer, E. Kuffel, E. McDermid.

[7] Cote, M., "A four-terminal co-axial pair Maxwell-Wein bridge for the measurement of self-inductance," Precision Electromagnetic Measurements Digest,2008. CPEM 2008. Conference on , vol., no., pp.714,715, 8-13 June 2008, doi: 10.1109/CPEM.2008.4574979

[8] Thompson, A.M., "AC Bridge Methods for the Measurement of Three-Terminal Admittances," Instrumentation and Measurement, IEEE Transactions on , vol.IM-13, no.4, pp.189,197, Dec. 1964, doi: 10.1109/TIM.1964.4313403

[9] Kuphaldt, Tony. University of Cambridge, Department of Engineering. Lessons In Electric Circuits: A free series of textbooks on the subjects of electricity and electronics. AC Metering Circuits [online]. 2000 - 2004 [cit. 2015-02-27]. Available from: http://www3.eng.cam.ac.uk/DesignOffice/mdp/electric_web/AC/ AC_12.html

[10] Sedláček, Radek. Measurement amplifiers and converters, vector voltmeter. Electrical Measurements and Instrumentation: Materials for Lectures [online]. [cit. 2015-02-28]. Available from: http://measure.feld.cvut.cz /en/system/files/files/en/education/courses/AE1B38EMA/lectures/Lecture_3.pdf

[11] Brooks, H.B.; Holtz, F.C., "The two-stage current transformer," American Institute of Electrical Engineers, Journal of the , vol.41, no.6, pp.389,398, June 1922 doi: 10.1109/JoAIEE.1922.6592459

[12] Betts, P.J., "Self-calibratable voltage transformer with part-per-million accuracy," Science, Measurement and Technology, IEE Proceedings - , vol.141, no.5, pp.379,382, Sep 1994, doi: 10.1049/ip-smt:19941068

[13] Slomovltz, Daniel, Leonardo TRIGO a Carlos FAVERIO. Two-stage current transformer with electronic compensation . [online]. UTE - Laboratory, Paraguay 2385, Montevideo, Uruguay, 2012, č. 1, s. 4 [cit. 2015-03-01]. Available from: http://acta.imeko.org/index.php/acta-imeko/article/viewFile/IMEKO-ACTA-01%282012%29-01-16/58

[14] Petr Voženílek, Vladimír Novotný. Elektromechanické měniče. 2. vyd. Praha: České vysoké učení technické v Praze, 2011. ISBN 978-800-1048-757.

[15] Souders, T. Michael. NATIONAL INSTITUTE OF STANDARDS AND TECHNOLOGY. Wide-Band Two-Stage Current Transformers of High Accuracy. Catalog of NIST Calibration Services [online]. 1972, p. 6 [cit. 2015-03-11]. Available from: http://www.nist.gov/calibrations/upload/im-21-4.pdf

[16] D. Slomovitz, H. de Souza, "Shielded Electronic Current Transformer," IEEE Trans. Instrum. Meas., vol. 54, no. 2, Apr. 2005, pp. 500-502.

[17] Haiming Shao; Feipeng Lin; Bo Liang; Xichang Qin; Shixiong Peng, "The development of a two-stage voltage transformer of 110/√3 kV and class 0.001," Precision Electromagnetic Measurements (CPEM 2014), 2014 Conference on , vol., no., pp.774,775, 24-29 Aug. 2014, doi: 10.1109/CPEM.2014.6898615

[18] Djokic, B.; So, E., "An Optically Isolated Hybrid Two-Stage Current Transformer for Measurements at High Voltage," Instrumentation and Measurement Technology Conference, 2005. IMTC 2005. Proceedings of the IEEE , vol.2, no., pp.1044,1047, 16-19 May 2005, doi: 10.1109/IMTC.2005.1604300

[19] Schneider, Michael. Metody měření činných a jalových výkonů. Praha, 2013. 52 s. Bakalářská práce. České vysoké učení technické v Praze. Vedoucí práce: Ing. Radek Procházka, Ph.D. Oponent práce: Ing. Jan Hlaváček, Ph.D.

[20] Srivastava, Anurag K. Phasor Measurement (Estimation) Units [online]. Washington State University [cit. 2015-03-22]. 59 p. Available from: https://www.eiseverywhere.com/file_uploads/b9c0cedfe296b5347ce0877fbfac3753_PMU_Relay_Schoolcopy.pdf. Presentation. The School of Electrical Engineering and Computer Science, Washington.

[21] Liang Du; Jin-kai Huang; Qun-ying Liu, "A Realization of Measurement Unit for Phasor Measurement Unit Based on DSP," Power and Energy Engineering Conference (APPEEC), 2012 Asia-Pacific , vol., no., pp.1,3, 27-29 March 2012 doi: 10.1109/APPEEC.2012.6307689

[22] Gajjar, G.; Soman, S.A., "A proposal for distributed architecture for synchronized phasor measurement unit," Power and Energy Systems (ICPS), 2011 International Conference on , vol., no., pp.1,7, 22-24 Dec. 2011, doi: 10.1109/ICPES.2011.6156634

[23] Yeong-Chin Chen; Jian-kai Lan, "Implementation of Power Measurement System with Fourier Series and Zero-Crossing Algorithm," Computer, Consumer and Control (IS3C), 2014 International Symposium on, vol., no., pp.601,604, 10-12 June 2014, doi: 10.1109/IS3C.2014.163

[24] Roddy, D., "A method of using Simpson's rule in the DFT," Acoustics, Speech and Signal Processing, IEEE Transactions on , vol.29, no.4, pp.936,937, Aug 1981 doi: 10.1109/TASSP.1981.1163629

[25] Acquitek. CompuScope 1610: Ultra-fast waveform digitizer card for PCI bus. [online]. 900 N. State St. Lockport, 2006, p. 5, March 31st 2006 [cit. 2015-03-28]. Available from: http://www.acquitek.com/data/acc_docsend.php

[26] Yokogawa Meters & Instruments Corporation. User's manual: Precision Power Analyzer WT3000. 383 s. Available from: http://tmi.yokogawa.com /us/products/digital-power-analyzers/digital-power-analyzers/wt3000-precision-power-analyzer/

[27] Velleman, Daniel, The generalized Simpson's rule. The American Mathematical Monthly 112(4), pp. 342-350. 2005. Available from : http://ezproxy.techlib.cz /login?url=http://search.proquest.com/docview/203817033?accountid=119841

[28] Havlíček, Václav a Ivan Zemánek. Elektrické obvody 2. 1. vyd. Praha: České vysoké učení technické v Praze, 2008, 368 s. ISBN 978-80-01-03971-7.

[29] Instrukcja obslugi, Stacjonarny mostek RLC. BR-2817. Shanghai MCP Corporation. nr indeksu: 104684. Wyprodukowano w Chinach. Importer: BIALL Sp. z o.o., Otomin, ul. Słoneczna 4 3, 80-174 GDAŃSK, www.biall.com.pl.

List of used devices

IT	**Isolation transformer**	CTU SN: I3-6754/01
AT1, AT2	**Autotransformers**	RFT Sparstelltrafo LSS 010
A – Agilent	**6 ½ Digital multimeter**	Agilent 34401A
V – HP	**6 ½ Digital multimeter**	Hewlett Packard 34401A
Shunt	**Shunt 1.007 Ω**	SN: 543 206
V – Metex	**3 ¾ Digital multimeter**	Metex M – 3890D
	Digitizer card	CompuScope 12100
L	**Measured reactor**	10 mH, 20A

List of abbreviations

ABF Analog band-pass filter

AC Alternating current

A/D Analog-to-digital converter

CEO Chief executive officer

CR Controlled rectifier

CT Current transformer

ČEPS Česká energetická přenosová soustava
(Czech Transmission System Operator)

DC Direct current

DFT Discrete Fourier transform

DSP Digital signal processing
Digital signal processor

F Filter

GPS Global Positioning System

HVD High voltage divider

MRI Magnetic resonance imaging

PC Personal computer

PMU Phasor measurement unit

PJM Pennsylvania New Jersey Maryland Interconnection
(American regional transmission organization)

ppm Parts per million

SC Squaring circuit

TM Timing module

TSVT Two-stage voltage transformer

TST Two-stage transformer

TSCT Two-stage current transformer

VT Voltage transformer

List of symbols

P_C	Active power (continuous)
P_D	Active power (discrete)
p_i	Instantaneous power value
p_{max}	Peak amplitude of instantaneous power
δ	Active power error or loss angle
φ	Phase angle
σ	Standard deviation
k_p	Unity power factor error
k_q	Zero power factor error
k_V	Voltage error coefficient
k_I	Current error coefficient or current ratio
k_U	Voltage ratio
ε_U	Voltage ratio error
ε_I	Current ratio error
β	Phase angle error
e_U	Fractional error of two-stage voltage transformer
e_I	Fractional error of two-stage current transformer
I_{1D}	Desired current (the primary current of the ideal instrument transformer)
I_{1Fe}	Current which represents core losses
$I_{1\mu}$	Magnetizing current
I_{10}	'Supply current' – vector addition of core losses and magnetizing current
Φ_μ	Magnetic flux

List of equations

Table of figures

Appendix A - CompuScope 1610

CompuScope 1610	
Selected electrical parameters and absolute maximum ratings	
Channels A and B	
Impedance	1 MΩ, 35 pF or 50 Ω; software selectable
Coupling	AC or DC
Single-Ended Input Voltage Range	± 500 mV, ± 1 V, ± 2 V, ± 10 V
Absolute Maximum Amplitude	1 MΩ Impedance: ± 15 V (continuous) 50 Ω Impedance: ± 5 V (continuous) ± 15 V (for 1 ms duration)
Sampling Rate:	MS/s: 10, 5, 2.5, 1 kS/s: 500, 200 , 100, 50, 20, 10, 5, 2, 1
Protection	1 MΩ Impedance: Diode Clapped 50 Ω Impedance: No protection
DC Accuracy relative to full scale input:	± 0.5 % of full scale
Acquisition memory	
Memory Sizes:	1M, 8M, 128 M, 512 M, 1G
Maximum Depth:	Up to half on-board memory per channel
Triggering	
Number of Trigger Inputs:	2 per card
Trigger Source:	CH A, CH B, EXT or Software
Slope:	Positive or Negative; software selectable
External trigger	
Impedance:	1 MΩ, 30 pF
Amplitude:	Absolute Maximum ± 15 V
Internal clock	
Source:	20 MHz Clock Oscillator
Accuracy:	± 50 ppm
External clock	
Maximum Frequency:	20 MHz, maximum using 2 x decimation filter (10 MS/s)
Minimum Frequency:	2 kHz
Termination Impedance:	50 Ω

Appendix B - CompuScope 12100

CompuScope 12100	
Selected electrical parameters and absolute maximum ratings	
Channels A and B	
Impedance	1 MΩ, 25 pF or 50 Ω; software selectable
Coupling	AC or DC
Input Voltage Ranges	± 100 mV, ± 200 mV, ± 500 mV, ± 1 V, ± 2 V, ± 5 V
Absolute Maximum Amplitude	1 MΩ Impedance: ± 15 V (continuous) 50 Ω Impedance: ± 5 V (continuous)
Sampling Rate	50, 25, 10, 5 MS in dual channel mode 100, 50, 20, 10 MS in single channel mode
Protection	1 MΩ Impedance: Diode Clapped 50 Ω Impedance: No protection
DC Accuracy relative to full scale input:	Depends on input range: ± 5 V and ± 100 mV; 1 % of full scale ± 1 V, ± 2V, ± 200 mV, ± 500 mV; 0.5 % of full scale
Acquisition memory	
Memory Sizes	1M, 4M, 8M
Maximum Depth	Single-channel mode: Full on-board memory Dual-channel mode: Up to half on-board memory per channel
Triggering	
Number of Trigger Inputs:	2 per system
Trigger Source	CH A, CH B, EXT or Software
Slope	Positive or Negative; software selectable
External trigger	
Impedance	1 MΩ, 30 pF
Amplitude	Absolute Maximum ± 15 V
Internal clock	
Source	100 MHz Clock Oscillator
Accuracy	± 50 ppm
External clock	
Maximum Frequency	100 MHz
Minimum Frequency	10 MHz
Termination Impedance	50 Ω

Appendix C – Measured reactor and measuring workplace

Three reactors borrowed from the Department of Electric Drives and Traction

Measured reactor is the biggest one on the left. Here it its label:

Measured reactor in detail:

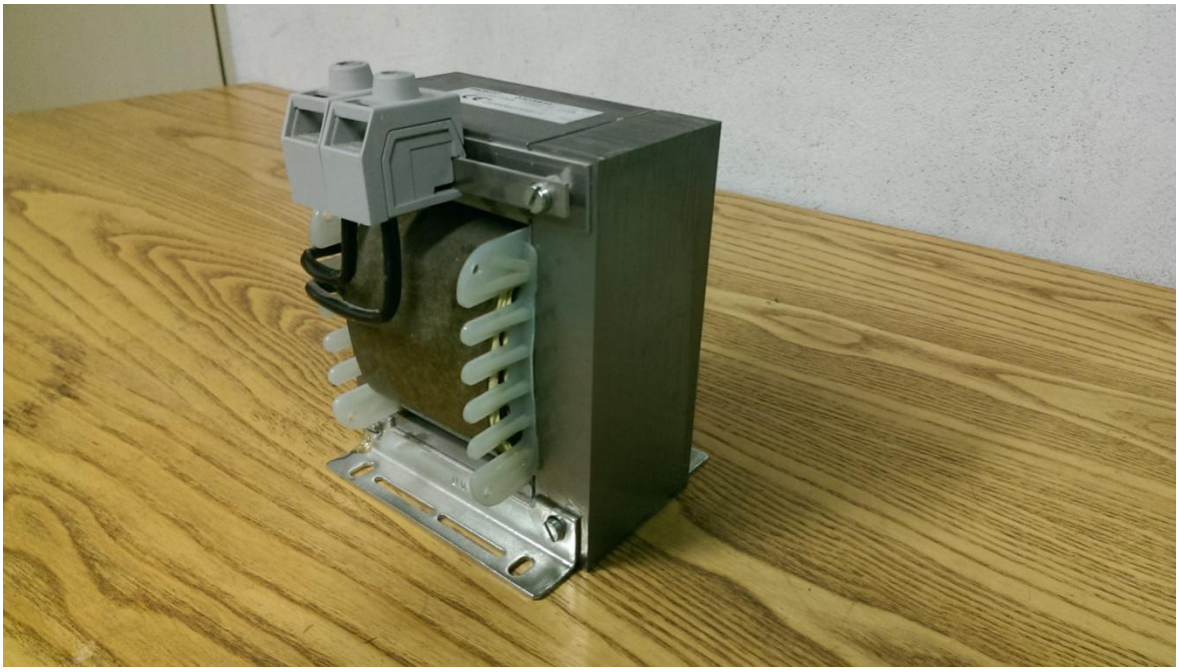

Measuring workplace:

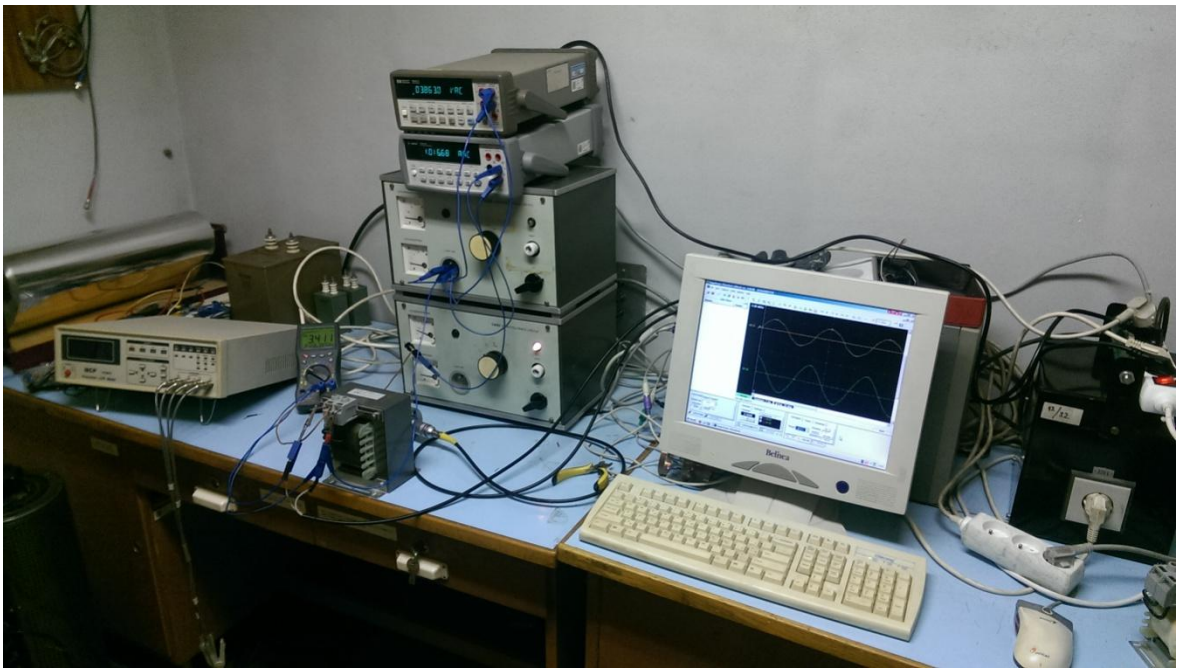

CD – ROM contents

/DT.pdf (thesis in pdf)

/Testing model

/Appendix D - Comparison of methods

/Appendix E – Trapezoid method using averaging

/Computing program

/Appendix F – Program for input modifications

/Appendix G – Computing program

/Data

/Voltage

/Current

/Photos

/Measuring workplace

/Reactors

/Measured reactor – detail

/Measured reactor – label